Seismic Assessment of Selective Retrofitting Technologies for Typical School Buildings in Jordan

***Thaer F. Zayadneh*[(1)] *Nazzal S. Armouti*[(2)]**

[(1)]Engineer, MSc, Jordan Engineers Association, E-Mail: t.zayadneh@jea.org.jo

[(2)]Associate Professor, Civil Engineering Department, University of Jordan, E-Mail: armouti@ju.edu.jo

ABSTRACT

Seismic assessment and retrofitting of typical school building are carried out using a finite element software package implementing the recent fiber based beam-column element approach taking into account the geometric and materials nonlinearities. The local intervention of element jacketing with steel plates and carbon fiber reinforced polymers (CFRP) sheets is compared with constructing new shear walls as a global retrofitting. The comparison addresses, as a first priority, the ability to apply these methods in our practical applications to ensure their effectiveness. Nonlinear static analyses procedures (NSP) are used to locate the seismic deficiencies based on elastic response spectra developed for site conditions. The study shows the effectiveness of constructing new shear walls in reducing the local seismic demands on deficient elements. The global stiffening considerably limits the interstory drift ratios achieving a predefined performance level. The distribution of stiffness and strength is also modified by lessening the irregularity of the structural system. On the other hand, local modifications using CFRP-strengthening shows a good alternative solution for enhancing the shear resistance of columns and drop beams with almost no contribution on increasing the deformation capacity through confinement due to high aspect ratio effect.

KEYWORDS: Shear Wall, Steel Plate, CFRP-Wrapping, fiber-based, Seismic performance, Nonlinear analysis.

INTRODUCTION

The building, as shown in Figure 1, is located in Maa'n, southern Jordan, 218 kilometers southwest of the capital Amman. The structural system information and description are listed in Table 1. The building consists of 4-story reinforced concrete floors with two main cores and beam-column elements. The building has relatively large openings with almost 50% of the external infill walls area. External infills are made of two brick stones with different sizes (100, and 150) mm separated by (50) mm with light isolation materials. The internal infills are light isolation walls with (100) mm bricks and plastering materials in both sides. The study will be considered as a bare frame structure (i.e. neglecting the effect of infill walls) trying to minimize the uncertainty and the complexity of the model [(FEMA 356, 2000), (Govalkar et al., 2014)].

Figure 1: King Abdullah II School for Excellence

Table 1: Building General Information

Building type	Low rise RC structure
Occupation	Puplic School
Number of stories	4
The areas of the ground, first, second, and third floor	916, 1140, 1008, and 848 m2, respectively

The foundation system is basically an isolated footing system while some are combined footings. Ground beam connections (moment resisting beams) of (300 × 500) mm2 are used to link the interior footings while elevated walls connect the external ones. Two main cores of (300) mm thickness are in the x-axis direction. The building also has a small elevator core with (200) mm thick walls.

The structural system of the school consists of a combination of beams, columns, and shear walls, which are used as lateral load resisting system (well known as dual system). Although the building was designed and built in 2010, the structure system has many critical issues related to its layout that affect the response of the entire structure.

Simple and regular structural plan is highly recommended in design of new buildings. Irregular structures are exhibiting coupled lateral/torsional response in which the deviation of the actual inelastic response from the presumed response calculated by simplified elastic analysis would be significant. For such reason, some critical issues are found important to clarify about the building under consideration and listed below (Fardis and Springer Link Online Service, 2009):

1. Lateral load resisting system

The building has relatively small structural columns that might be designed mainly to carry gravity loads. For instance, the only bracing against horizontal forces and displacements is a reinforced concrete elevator and stairway shaft. These walls are placed very asymmetrically at the corners of the building. A large eccentricity between the center of mass and resistance is expected. Twisting in the plan will lead to large relative displacements in the columns. As a result, punching shear failure is expected. By having a glance on the lateral load resisting system configurations, we could observe the following:

1. Structural walls are not arranged in the two orthogonal horizontal directions but rather concentrated along one direction.
2. Indirectly supported beams (i.e. indirect supports of some beams on others) introduce significant uncertainty by the interactions of such beams through torsion.
3. Since the diaphragm system is a one-way ribbed slab, major beams are mainly constructed perpendicular to

the rib direction only.

4. The arrangement of columns in the plan is irregular but along both principal directions. Beams are distributed between columns in one direction since the diaphragm system is ribbed one-way slab. This could lead to a non-uniformly distributed seismic force and deformation.

2. Plan Symmetry and Regularity

The structural system and the mass distribution are asymmetric with respect to two orthogonal horizontal axes. In such case, a rotational component of the ground motion will be significant. The rotational component arises from the differences of the translational components along both horizontal axes. Such difference in the displacement between opposite sides of the floor generates what is called stiff and flexible sides behavior. Torsional response imposes large displacement demand in one side (i.e. flexible side) which may yield earlier than the opposite side (i.e. the stiff side). The term "static eccentricity" is used to measure the lack of symmetry in plan. ETABS® 2015 software is used to locate the centers of mass and resistance as shown in Figure 2. The results show that the structural system of the school is irregular as shown Table 2.

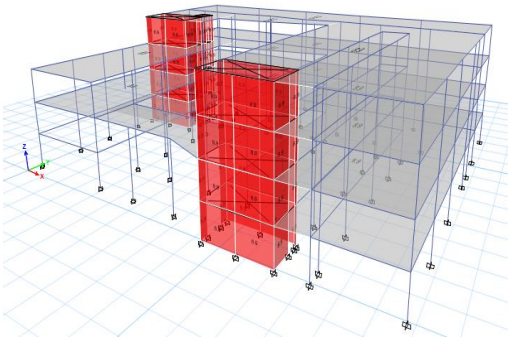

Figure 2: Modeling the School Building Using ETABS® 2015

Table 2: Centers of Mass and Resistance of King Abdullah II School

Story Diaphragm	Static eccentricity	
	$\mathbf{e_x}$	$\mathbf{e_y}$
	m	m
Story4	8.33	7.10
Story3	7.41	6.27
Story2	7.30	5.83
Story1	7.31	6.17

e_x Static eccentricity in X -direcion

e_y Static eccentricity in Y -direction

3. Geometry, Mass, and Lateral Stiffness Regularity with Elevation

A point load of 1000 kN is applied near the center of resistance (Basu and Jain, 2004) trying to minimize the effect of torsion and to get a uniform drift over all nodes in each floor. The lateral stiffness of each floor is calculated using the simple spring formula ($k_i = F/\Delta_i$) where k_i(kN/mm), F(kN), and Δ_i(mm) are the stiffness, applied horizontal force and lateral drift associated with level i, respectively . The lateral stiffness values are (in kN/mm) 1658, 919, 810, and 823 for the ground, first, second and third floor, respectively.

According to ASCE/SEI 7 (2010), a building is characterized to have a soft story irregularity if the lateral stiffness of specific story is less than 70% of that in story above or less than 80% of the average stiffness of the stories above. Obviously, this irregularity does not exist in our case because the stiffness is decreasing with elevation. On the other hand, mass irregularity is evaluated between the ground and first story (i.e. excluding the roof) in which the area of each floor is considered as an indication of mass. The mass ratio is less than 1.25 where the critical value is 1.5. The geometric irregularity of the school could be easily seen in the upper floor (i.e. the roof) where a sudden ending of lateral load resisting elements in one side of the building takes place. This type of irregularity exists if the horizontal dimension of the seismic force–resisting system in any story is more than 130% of that in an adjacent story which reached 180% in the building under consideration. Finally, the school is not suffering from in-plane discontinuity in vertical lateral force-resisting elements or discontinuity in capacity (Weak story irregularity) (ASCE/SEI 7, 2010).

SEISMIC ASSESSMENT OF THE BUILDING

This study will adopt the nonlinear fiber model, which is used to model the beam-column elements in SeismoStruct software (Seismosoft, 2014). Knowledge factor of 1.0 will be selected to achieve the BSO (FEMA 356, 2000). Columns are assumed fixed at their bases. The factored ultimate loads are taken as 10.5 kN/m^2 for slab, 15.0 and 9.5 kN/m for external and internal infills, respectively.

Since no tests were performed, the compressive strength of concrete, f_c', yield strength of longitudinal Reinforcement steel, f_y, and yield strength of transversal reinforcement steel, f_{yv}, were taken as 25, 420, and 280 respectively.

The earthquake design data are listed in Table 3. The elastic design response spectrum for of 5% equivalent viscous damping and a 10-percent probability of being exceeded in 50 years could be now drawn.

Table 3: Earthquake Design Data as Required by UBC (1997)

Earthquake Design Data	
Seismic Importance Factor[1], *I*.	*I=1.25*
Occupancy Category.	Schools = *III*
Seismic Zone Factor Z.	*Z=0.15*
Seismic Coefficients C_a and C_v.	0.22 and 0.32 respectively.
Site class[2].	Soil Profile, S_D
Control Periods T_s and T_o.	0.75 and 0.15 respectively.

The effective stiffness will be taken as one-half the gross one (i.e. E_cI = 50% $E_c.I_{gross}$) where the modulus of elasticity, E_c, is evaluated from the formula [$E_c = 4700\sqrt{f_c'}$][3] (ACI 318, 2014).

The building was analyzed with two different slab configurations: a) equivalent truss elements (Mpampatsikos V. , 2008) and b) rigid diaphragm. For equivalent truss approach, two X-diagonal trusses connect the slab corners by means of their axial stiffness. The computational models using SeismoStruct software are shown Figure **3**a, 3b. Table 4 illustrates the numerical results of the eigenvalue analyses.

[1] Section 11.5.1 of ASCE 7 (2010).
[2] No test on site information
[3] Units are in MPa.

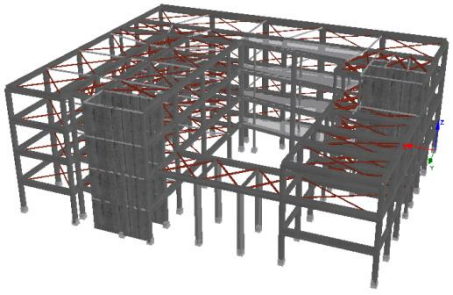

a)

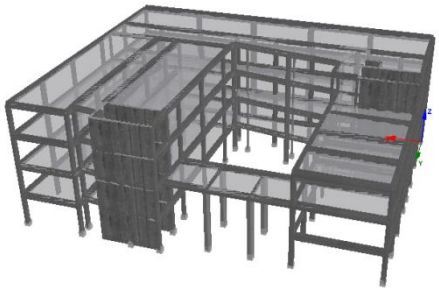

b)

Figure 3: Models of King Abdullah II School a) Equivalent truss b) Rigid diaphragm

Table Error! No text of specified style in document.**4: Modal Mass Percentages.**

Mode	Period (sec.)	Mass participation %		
		X	Y	Z
Equivalent Truss				
1	0.56	0.17	**82.49**	0.09
2	0.29	**69.54**	0.34	1.57
3	0.20	0.25	3.28	12.60
4	0.19	0.25	8.20	0.69
Rigid diaphragm				
1	0.55	0.13	**82.82**	0.15
2	0.37	**29.82**	0.34	44.59
3	0.21	**41.93**	0.04	29.35
4	0.18	0.11	12.43	0.36

The number of modes required to capture 90% of the modal mass varies from 15 for translation along x-direction, 4 for translation in y-direction and 13 for the rotation about z- direction. However, the first three modes capture about 70-80% of total cumulative mass along the principal directions.

In NSP, the model of Mander et al. (1989) will be selected as concrete model. The confinment factor will be automatically calculated by the program. Wide-column approch is used to model the shear walls. Monti-Nuti steel model (Fragiadakis et al., 2008) will be adopted as a steel uniaxial stress-strain relationship. Columns are assumed fixed at their bases. Unreduced sectional moment of inertia is taken since concrete cracking is considered by the concrete stress-strain relationship using the fibre element approch. All strutural elements are modeled using the avaiable drawing sheets considering their reinforcemnt. The ultimate weight of the structure is assigned as an additional mass per unit length of the element (ton/m). Many different element classes are used in the software.

The study implements the recent fiber beam-column element approach. Inelastic force-based frame element type (termed by infrmFB) will be chosen to model a member of space frame with geometric and material nonlinearities. In the case of rigid diaphragm model, The lack in regularity of the structural frame makes the amount of mass in X – direction less than 42% in the 3rd mode shape and the rotational component to reach 44% in the 2nd one. Translations along Y-axis, as shown in Figure **4**a, will be taken as first modal pattern for $T=T_1=0.55$ *sec.* in which 83% of the mass is dominated by this mode. For X- direction, the structure will be pushed for the 2nd and 3rd modes to capture 71% of the mass in that direction. The torsional effect is clearly seen in these two modes as shown in Figure **4**b and 4c.

Tow lateral load distribution patterns (FEMA 356, 2000): modal and uniform, could be computed using the formulas listed below and described in the work of Nicknam et al. (2008). These values could be easily extracted from the software as shown in Table 5.

1. First mode lateral load pattern(C_{vi}) where Φ_i and m_i are the first mode shape and mass value for the *i*th node, respectively.
   $C_{vi} = \frac{\Phi_i \times m_i}{\sum_{i=1}^{n} \Phi_i \times m_i}$
2. Uniform lateral load pattern (C_{mi})
   $C_{mi} = \frac{m_i}{\sum_{i=1}^{n} m_i}$

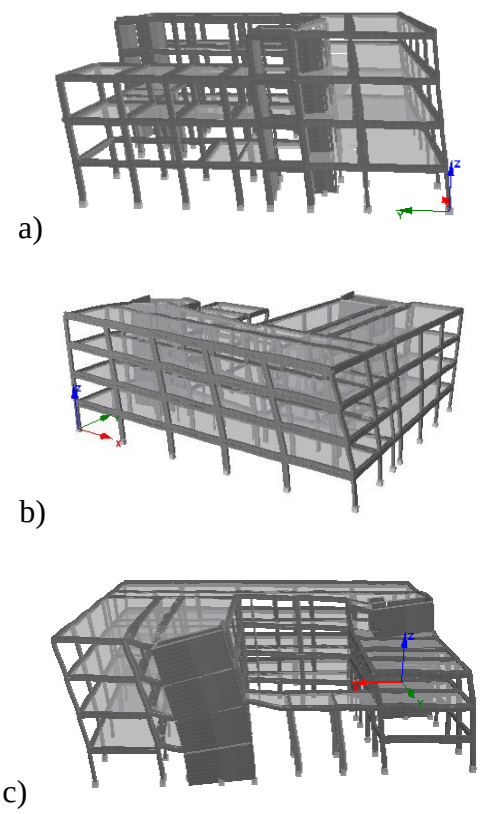

Figure 4: a) 1st, b) 2nd, and c) 3rd Shape Modes of King Abdullah II School, *T= 0.55, 0.37,* and *0.21 sec* respectively.

Table 5: Lateral Load Distribution Calculations where T =T1= 0.56 sec for Y direction.

Node	m_{yi} (ton)	Φ_{iy}	$\Phi_{iy}.m_{yi}$
n54	4.0	2.14E-06	8.60E-06
n53	17.4	2.40E-06	4.18E-05
n52	17.4	2.27E-06	3.95E-05
n51	64.7	2.75E-06	1.78E-04
n50	72.1	2.66E-06	1.92E-04

The capacity curve is generated by the software for the multi-degree of freedom (MDOF) system of the school using the roof displacement and corresponding base shear. Figure 5 shows the capacity curves of rigid diaphragm model along both principal directions. Along the X-direction, both modal displacements corresponding to the 2nd and 3rd mode shapes were selected (i.e. *T=0.37 and 0.21 sec.*). Since the lack of symmetry in plan is obvious, larger displacements are developed in the flexible direction (i.e. Y-Direction) where a stiffer response is observed along the X-direction. The response of the structure differs based on the lateral load patterns for both models. The modal pushover curves are generated proportional to the shape of the fundamental mode of the considered direction. These curves demonstrate the more critical response under a constant horizontal load. The maximum capacities are usually obtained from the uniform lateral load calculated proportional to the mass of each node ($m_i/\sum m_i$). It is worth mentioning that a significant uncertin weak response appears along the 2nd modal shape for rigid diaphragm model where the translational mass is only about 30% of the total mass along that direction. This weak response is due to the torsional effect of that mode (i.e. T_2 = 0.37 sec.) since 45% of the total mass are rotating about the vertical axis. Such torsional efffect is clear in Figure 6.

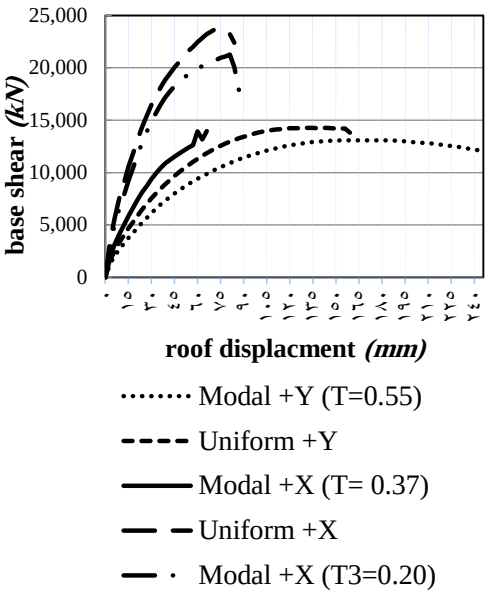

Figure 5: Roof Displacement versus Base Shear for Rigid diaphragm Model

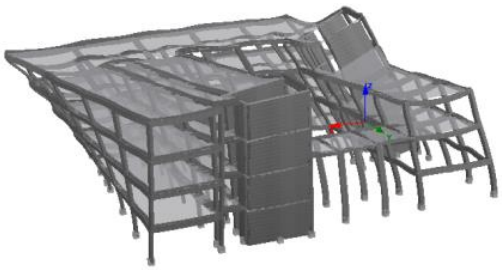

Figure 6: Modal Pushover for T_2 = 0.37 Sec.

Capacity spectrum method (ATC, 1996) will be used to evaluate the maximum displacement of the school (i.e. the performance point) under the predefined seismic hazard level (i.e. 10%/50 years). The procedure is extensively discussed in FEMA 440 (2005). Mode shapes and associated periods of vibration are listed in Table 6. Rigid diaphragm model will be adopted in the performance points calculations. For rigid diaphragm model, the more critical modal pushover anaysis will be selected : the modal pushover anaysis in Y (*T = 0.55 sec.*) and X (*T=0.37 sec.*). Figure 7 shows the graphical calculation of the performanc point (Method A) along both directions. Other related parameters (ATC, 1996) are listed in Table 8.

Table 6: Mode Shapes and Associated Periods

Slab Modeling Approach	Mode Numb-er	Directi-on	Period of Vibratio-n (sec.)
Rigid diaphragm model	1	Y	0.55
	2	X	0.37

Performance point (d_i, a_i) could be estimated through intersecting the effective period T_{eff} with the reduced ADRS Demand (i.e. ADRS, B_{eff}), then vertical line is constructed to the ESDOF capacity to form a new point of intersection (d_i, a_i). The procedure is repeated until convergence. The coordinates of the performance point (PP): (spectral displacement, spectral acceleration) in Figure 7 are then inverted to nodal displacement and base shear (i.e. Pushover curve representation).

Performance points for both directions are listed in Table 7. The assessment of that performance point could be now done as shown in Figure 8 by defining the material strains listed in. where:

V_{pi} (kN)	The base shear value of the performance point for MDOF system.
$d_{cn,pi}$ (m)	The roof displacement of the performance point for MDOF system.
a_{pi} (g)	The acceleration value of the performance point for ESDOF system in ADRS Format.
d_{pi} (m)	The corresponding displacement value of the performance point for ESDOF system in ADRS Format

The results show that many structural elements reach the ultimate crushing strain of the confined concrete far away from the performance points. The mechanism of strong beams- weak columns is obvious where columns yield before beams as shown in Figure 8a.

By achieving the basic safety objective as a rehabilitation objective, the following dual rehabilitation goals are met:

- LS building performance level (SD in Eurocode 8 (CEN, 2010)) under the BSE-1 Earthquake Hazard Level, and
- CP building performance level (NC in Eurocode 8 (CEN, 2010)) for the BSE-2 Earthquake Hazard Level

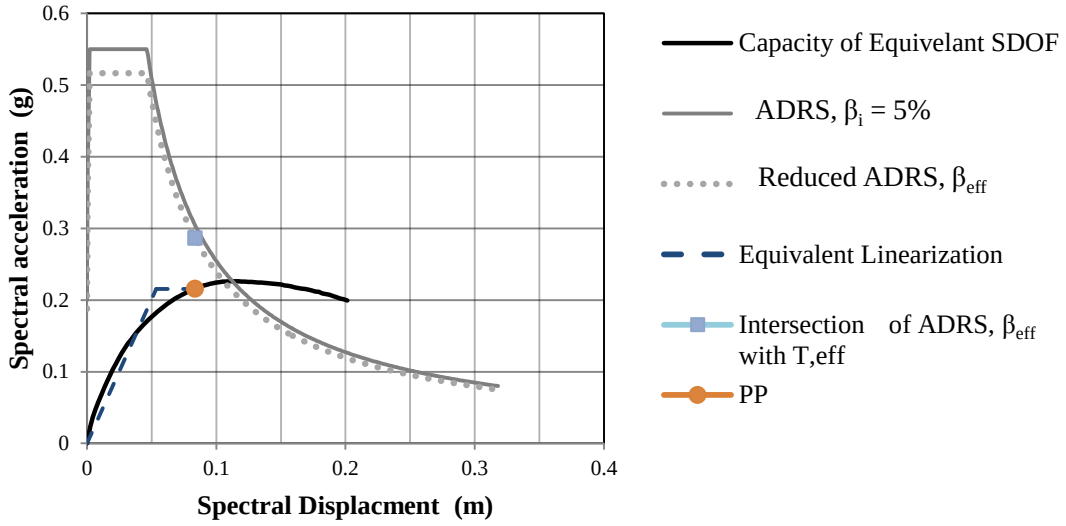

(a) Y- Direction

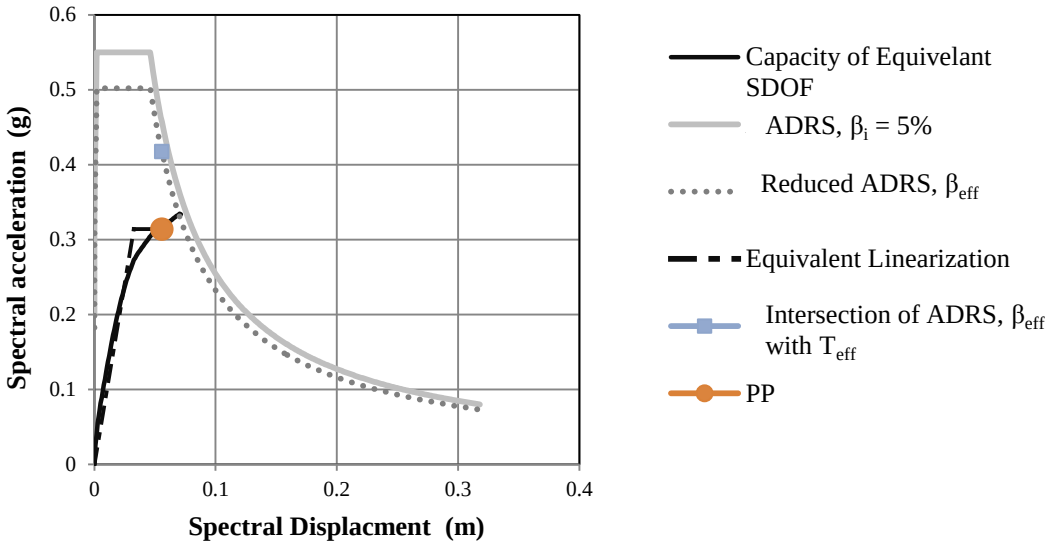

(b) X- Direction

Figure 7: Graphical Calculation of Performance Point along: a) Y-Direction and b) X-Direction

Table 7: Performance Points for both Directions.

	Performance Points (PP)			
	Standard Capacity Format		ADRS Format	
Direction	V_{pi} (kN)	$d_{cn,pi}$ (m)	a_{pi} (g)	d_{pi} (m)
X	12500	0.064	0.314	0.056
Y	12207	0.108	0.216	0.084

Table 8: Capacity Spectrum Method – Method A: Related Parameters (ATC, 1996)

Parameters	Description/ value
Spectral representation of the ground motion.	
Initial Damping, β_i	5%
Foundation Damping, β_0	ignored (i.e. $\beta_0 = \beta_i$)
Conversion to ADRS Demand Formulas	$S_{di(ADRS)} = S_{ai}\left(\frac{T_i}{4\pi}\right)^2 \times 9.81\ (m)$ $S_{ai(ADRS)} = S_{ai}$ (g)
MDOF Capacity curve (i.e. pushover analysis results).	
Conversion to ADRS Capacity Formulas for equivalent single degree of freedom (ESDOF) system.	$S_{di(ADRS)} = \frac{d_{cn}}{\Gamma_i \times \phi_{cn}}(m)$ $S_{ai(ADRS)} = \frac{V_i}{\Gamma_i \times M_i \times g}$(g)
• Capacity spectrum method (also known as Equivalent Linearization)	
Initial Period, T_0	$T_0 = \sqrt{4 \times \frac{\pi^2 S_{d1}}{S_{a1} * 9.81}}$ (*sec.*)
Initial Performance Point (maximum acceleration, a_{pi}, and displacement, d_{pi})	Engineering Judgment.
Developing a bilinear representation[4] of the capacity spectrum as shown in Figure 4-15a.	$d_y = \frac{Area + d_{pi}a_y + a_{pi}d_{pi}}{a_{pi}}$ where Yield displacement, d_y, yield acceleration, a_y, and initial period, T_o.
Ductility, μ.	$\mu = \frac{d_{pi}}{d_y}$
Post-elastic stiffness, α.	$\alpha = (a_{pi} - a_y)/(d_{pi} - d_y)/(a_y/d_y)$

Parameters	Description/ value
Effective period, t_{eff}, and effective damping, β_{eff}	Section 6.2.1 and 6.2.1 respectively in FEMA 440 (2005)
CSM: Procedure A (Direct Iteration).	
Adjusting the initial demand ADRS to account for the effective damping, β_{eff} (reduced ADRS, β_{eff}) as shown in b.	$(S_{a\beta})_\beta = \frac{(S_{ai})_{(ADRS)}}{B(\beta_{eff})}$ $B(\beta_{eff}) = \frac{4}{5.6 - Ln(\beta_{eff})}$

[4] Area under the capacity curve to the maximum displacement point (i.e. performance point, d_{pi})

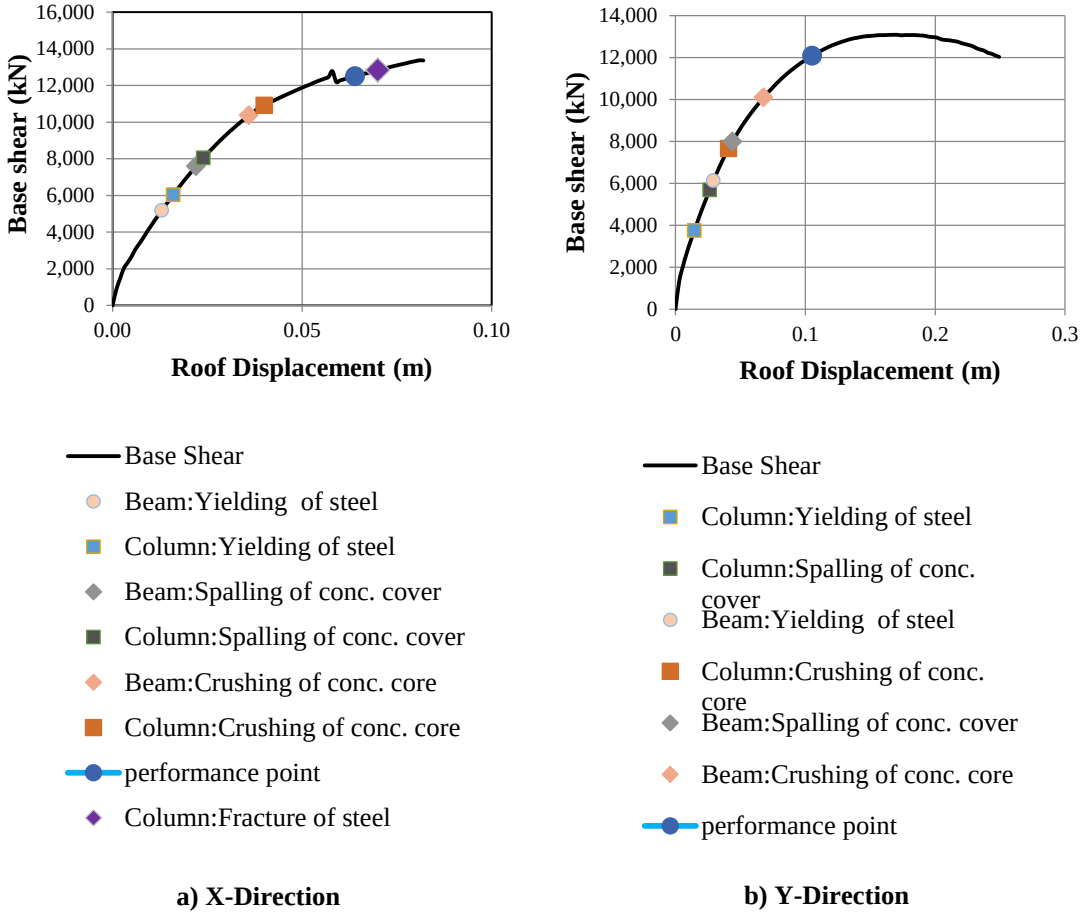

a) X-Direction **b) Y-Direction**

Figure 8: Strain Values at Performance Point for a) Y-Direction and b) X-Direction

Table 9: Different Strain Parameters[5] Used in Assisting the Performance

Material Strains Parameter	Typical Value
Spalling of concrete cover	-0.002
Crushing of concrete core	-0.006
Yielding of steel	+0.0025
Fracture of steel	+0.060

Life safety performance level to be verified using SeismoStruct software (Seismosoft, 2014) by which the total chord rotation and shear strength capacities are automatically calculated at NC performance level.

The local chord system of the beam-column element shown in Figure 9 will be used to describe the element action directions and notation (shear, chord rotation, ..etc.). For example, The notation CR(2) represents the chord rotation about axis number (2) and V(3) represents the shear calculated along axis (3).

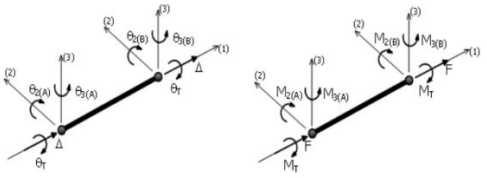

Figure 9: The Local Chord System of the Beam-Column Element Implemented in SeismoStruct

[5] See Section 6.4.3.1 : Usable Strain Limits in FEMA 356 (2000)

Deformation-controlled actions could be evaluated through examining the chord rotations at element ends. The chord rotation demands and capacities at performance points for both pushover directions are shown in Figures 11 for columns. The results show a satisfactory level of ductile capacity in terms of chord rotation under the specified seismic hazard level where no element has reached the capacity until the performance point fot both directions as shown in Figure 10 for Y direction.

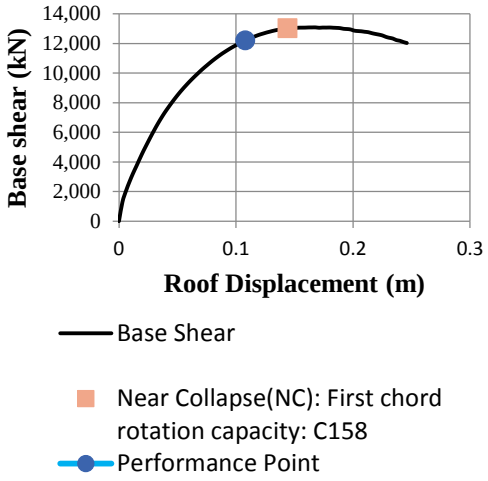

Figure 10: Chord Rotation Capacity Check (Y-Direction) Using Eurocode 8 (CEN, 2003) for NC

Table 10: Walls Local Shear Forces at Selected Point: Y-Direction

Wall #		I(2)/I(3)	V2 (kN)	V3 (kN)	Local Loading Direction
First floor	1	81	12	22	2
	2	81	1	660	3
	3	81	41	84	2

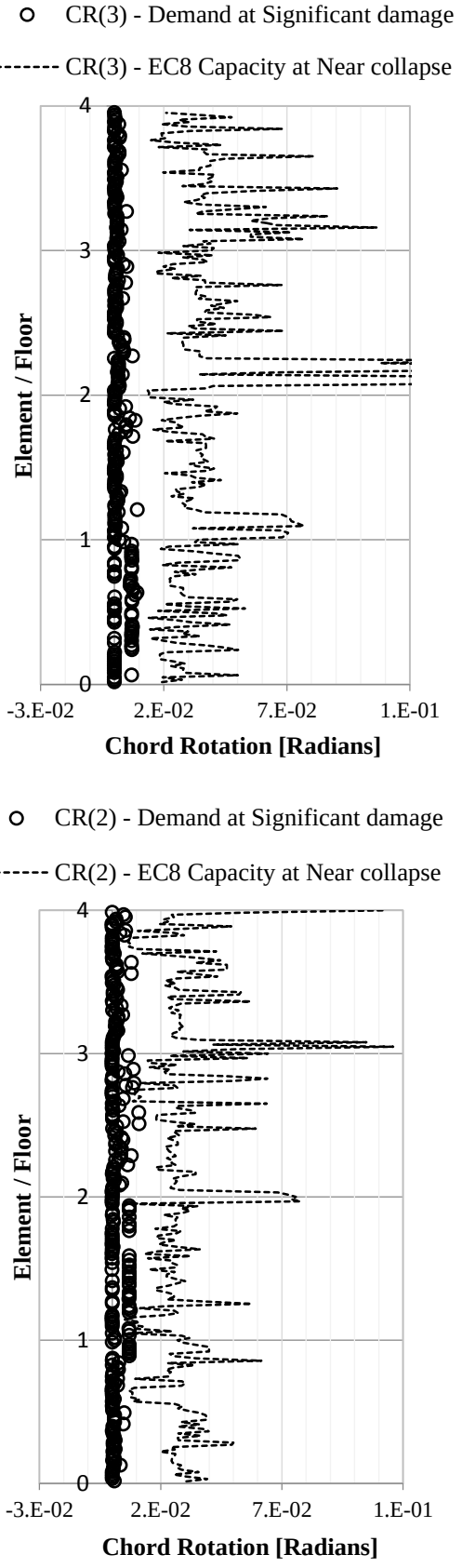

Figure 11: Columns Chord Rotation Demands and Capacities: Y-Direction

Since the accuracy of our model (i.e. fiber nonlinear flexure model) is highly sensitive to the shear demand (i.e. the brittle response), shear capacities evaluated at the performance point are to be compared with corresponding demands. The results show that few elements have reached the capacities along the axis number 3 for both directions of loading (i.e. X and Y). This is also clear when considering these values in beams where the numbers of elements at their respective strength are shown in and 4-28.

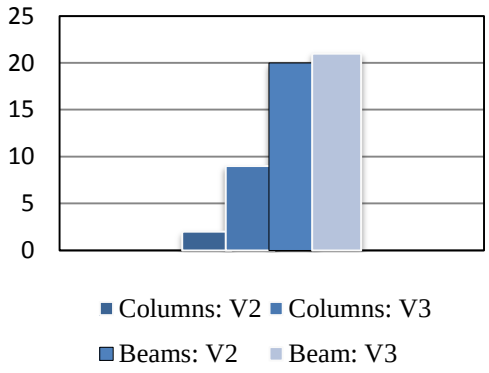

Y Direction

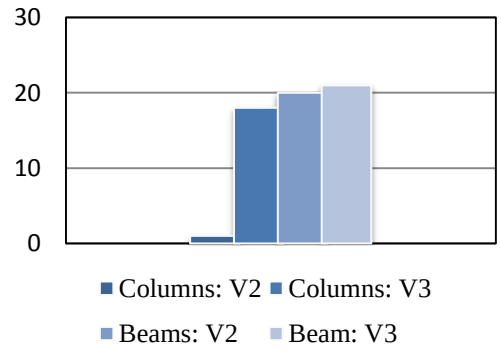

X Direction

Figure 12: Numbers of Elements reach their Respective Capacities

The model appears to be highly unsymmetrical. The consequence of this is that loads in the Y-direction can produce substantial deformations in the X-direction, and vice versa as shown in and 4-19[6]. A particular wall is selected for analysis like wall number 6 in
Table 10 where the moment of inertia is about 544 times as stiff about the local axis (2) as in the local axis (3). The load about the local axis (2) produces very large shear force along the opposite direction (i.e. local axis (3)). Such illustration could be easily seen by observing the local shear forces for both global directions in Table 4-19. It is also worth mentioning that almost all shear walls are aligned in one direction.

When the nonlinear static procedure is adopted to capture the responce of multistory buildings, the assessment of seismic performance would be the maximum interstory drift ratio ($(\Delta_{i+1} - \Delta_i) / L_{i+1}$) in percentage (Seo et al., 2015) where other ductile and forced actions should be also verified (i.e. chord rotation and shear).

Figure **13** and Figure **14** show the maximum story drift ratios and displacement along Y and X directions, respectively. The structure should maintain strength and ductility to accept that the performance limit of LS- for example- is met (FEMA 356, 2000). These measures of performance could be seen in Table **11** in terms of drift ratio. Other LS performance measures are:

- Extensive damage to beams.
- Spalling of cover for ductile columns
- Limited buckling of reinforcement.

[6] A point within the pushover curve is randomly selected for both directions.

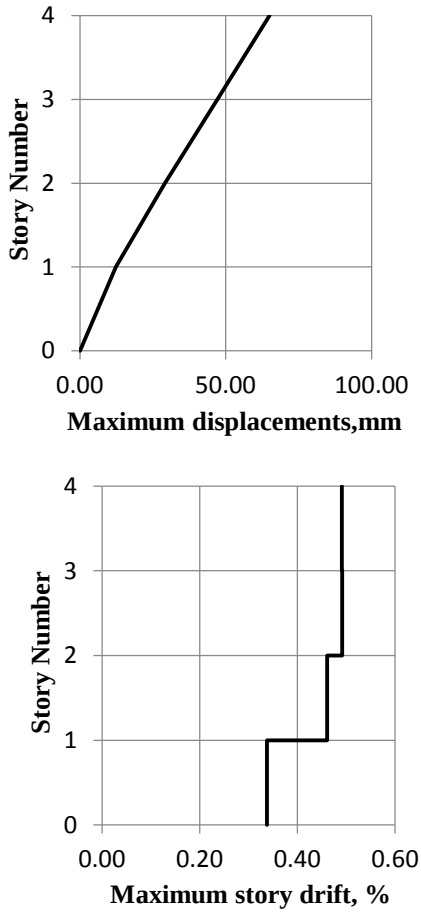

Figure 13: The Maximum Global Displacements and Interstory Drifts at the Performance Point for X-Direction

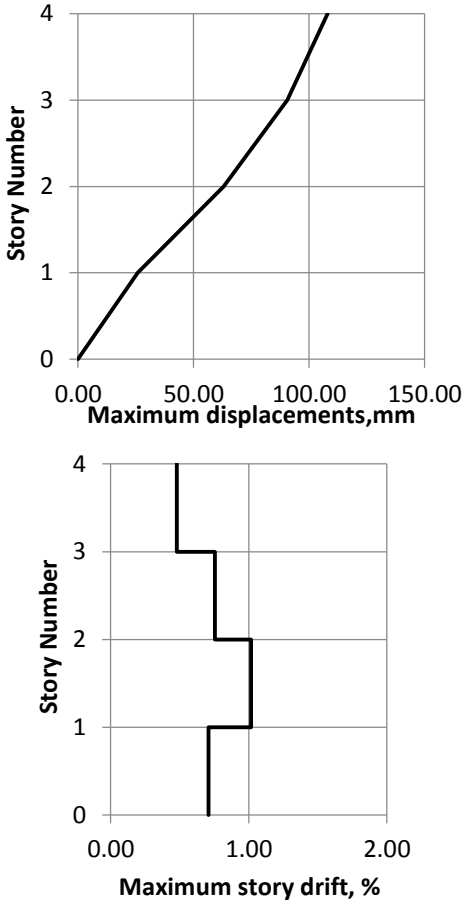

Figure 14: The Maximum Global Displacements and Interstory Drifts at the Performance Point for Y-Direction

Table 11: Structural Performance Levels in terms of Drift Ratio (FEMA 356, 2000)

Element	Structural Performance Levels		
	CP	LS	IO
Concrete Frames	4%	2%	1%
Concrete Walls	2%	1%	0.5%

The structure could not stand the maximum loading of the imposed hazard without violating the performance measures even at the minimum requirement of life safety performance level for such important buildings like schools. A more critical scenario will be faced when considering the actual materials properties and strength or introducing the knowledge factor of reducing the strength by 25% if the enhanced rehabilitation objectives is needed to be met.

As a result, the building needs to be retrofitted and enhanced to be operational or at least achieving the immediate occupancy (IO) limit state under these moderate seismic demands of basic safety earthquake 1(i.e. 10%/50 years).

Buildings at IO performance level are expected to sustain no damage to their structural elements and only minor damage to their nonstructural components. As a result, it is allowable to reoccupy the building.

SEISMIC REHABILITATION AND RETROFFITING OF THE BUILDING

Local and global modifications of the school structural system are suggested to upgrade the seismic response and overcome the seismic deficiencies. Even though the structure is asymmetric and the torsional response is obvious, the main problem that needs to be addressed is the brittle failure mechanisms of some elements since the model is not accurate up to those points of failure. The flexural behavior maintains strength and ductility for corresponding demands along Y direction with some reduction in strength for X direction where no chord rotation capacity (at near collapse) is reached. Other indications for such ductile behavior is that many elements are yielding and others are reaching the confined concrete core fracture strain (indicative value of (-0.006) is assumed). Therefore, the objective of this systematic retrofitting is to (1) ensure that no shear capacity is reached up to the performance point and (2) limit the yielding of reinforcing steel and concrete fracture to an acceptable limit. The effects of different retrofitting strategies are also investigated in terms of interstory drift ratios.

The structural system of the school is retrofitted to achieve the Immediate Occupancy (1-B) performance level (Damage Limitation (DL)) under the Basic Safety Earthquake-1 (BSE-1:10%/50 years) imposed by the selected design response spectra. However, such performance level is normally associated with less hazardous seismic action (i.e. 20%/50 years). Earthquakes with high probability of exceedance, for example: 20%/50 years, are less destructive and more likely to happen during the lifetime of the structure than others are (i.e. BSE-1). In other words, building performance limit is less demanding when it is associated with high intensity earthquake. The general requirements of the selected performance level are listed in Table 12.

Global and local interventions are implemented to upgrade the strength, stiffness and ductility of structural elements where they are needed. The effects of these retrofitting interventions on the global response are shown in Figure 15.

Table 12: Performance Level Objective

Performance level	Overall Damage	Risk	The Significance of Repair	Effect on Some Concrete Structural Systems	
				Frames	Walls
Immediate Occupancy	No change in strength and stiffness, light damage, no permanent drifts, and some minor hairline cracks appear.	Low or no risk of life threatening, and fire protection is maintained.	The repair is feasible where some minor hairline cracks are needed to be repaired.	Minor hairline cracks, limited yielding of components with no crushing of concrete (strains < 0.003), and 1% transient drifts.	Minor hairline cracks and 0.5% transient drifts.

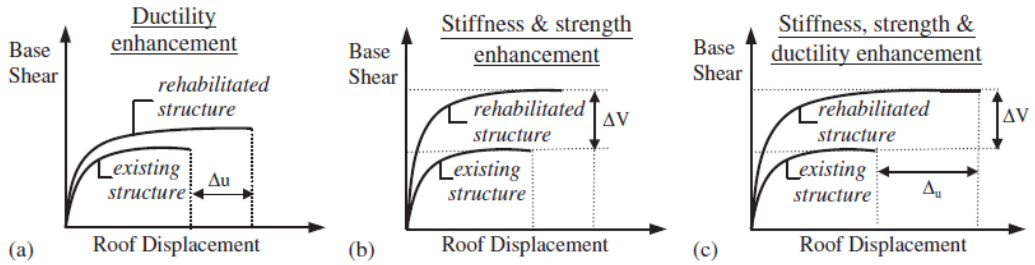

Figure 15: Effect of Different Retrofitting Interventions (Thermou and Elnashai, 2008)

It should be clear that the local rehabilitation methodologies implemented in this study are "selective" modifications that enhance a certain aspect of seismic behavior and not necessary (or not guaranteed) to improve others. Local improvement of strength and ductility is an effective and economical solution when a few deficient structural components are identified. In this strategy, the original overall structural configuration is maintained.

Elements jacketing with Carbon Fiber-Reinforced Polymers (CFRP)) and steel plates are investigated. These retrofitting technologies could be introduced to those elements who have (1) insufficient shear strength (2) strain values beyond the concrete crushing or steel yielding.

Elements are mainly jacketed with steel plates and CFRP sheets to provide additional shear reinforcements oriented in the direction of shear forces. The contribution of these jackets on displacement capacity (i.e. ductility) through confinement is sensitive to the section geometric properties and bonding schemes. Since these jackets practically stop before the end connections, they are not intended to enhance the flexural capacity of the retrofitted members (i.e. no change in structural stiffness). Enhancing the ductility through confinement is attained by jacketing the full perimeter of the cross section which is only applicable to isolated columns. Jacketing external vertical elements could cause a little disturbance as it needs to cut the continuity to the surrounding system. The aspect ratio of the strengthened section is another important issue since these jackets tend to buckle and lose their bonding strength. This is even more critical in jacketing rectangular shaped sections with steel plates. Limiting the global displacement demands by minimizing interstory drifts could be effectively gained through adding stiffness. Adding stiffness needs to jacket the regions of maximum moments (i.e. foundations and slab connections) which is not possible with these types of light jacketing. As a result and by having a constant stiffness distribution, the horizontal load distribution will not significantly change where the dominant behavior will be the torsional one.

The local modifications are highly recommended with limited deficient members -as in our case- if they come to enhance the related structural aspect of enhancing the shear capacity and delaying the concrete fracture. Providing that desired enhancement without major disturbance is another advantage. Since the local interventions of steel jacketing and CFRPs wrapping come to enhance a selective seismic capacity where no change is considered among others, there is no sense to develop comparison schemes (in terms of the global capacity response, for example) with other technologies.

In the case of global retrofitting, seismic demands on existing structural members are reduced to levels below the corresponding capacities. As a result, many elements are not required to be upgraded to such demands but others who have insufficient capacities under the gravity loads do. In this case study, some of those elements reached their respective shear strength in the beginning of pushover analysis. This could make the global interventions (i.e. inserting shear walls) inadequate if they do not alter the gravity load actions on these elements especially the horizontal ones (i.e. beams). In other cases, local retrofitting technologies are of significance (Pinho, 2000).

Constructing new shear walls provides both strength and stiffness to the overall structural response. The significance of such rehabilitation strategy is to get use of such new stiffness in reducing the irregularity of the school since the inelastic deformation demand is not uniform along both principal directions. This torsional effect could not be totally removed for many reasons since (1) the overall structural plan is one of the irregular shaped structures (i.e. re-entrant corner building) and (2) the mass and stiffness are not constant through the elevation. It could be impossible if these global interventions come to sustain the gravity loads and serve those elements with inadequate shear capacity.

The solution of balancing the distribution of stiffness and strength achieves many other strategies as it provides:

- Stiffness in order to improve the ductility. The school could not maintain ductility about the strong axis (i.e. X-direction) then a strength reduction is generated even before the performance point, and
- Strength along the flexible direction (i.e. Y direction) where many elements have reached the fracture strain of confined concrete and reinforcing bars.

Selecting the global interventions as a rehabilitation solution should be discussed with care since a massive disturbance to the existing system is expected altering the entire structural layout especially the connecting regions and openings. This could be a major threat if the current condition of the building is weak and needs repair. It would be also important to highlight the need of constructing new foundation system or modifying the existing one to sustain the loads form new shear wall elements.

Addition of shear walls usually comes to limit the global drift to acceptable limits (i.e. the performance indices). This would be significant for structures that suffer from extensive flexural failure (or damage) which could be estimated through the formulation of chord rotation capacities and remarkable fracture of many vertical elements. In our case, the flexural behavior is relatively maintained by the structure with small values of interstory drifts. All of these interpretations are based on the predefined BSE-1. Therefore, the local rehabilitation methods should be considered first in this study.

Steel Jacketing

A continuous thin plate jacket, as shown in Figure 16, is introduced for those shear deficient elements. The shear strength to be sustained by the jacket (V_j) is calculated by Equation 5-1 (CEN, 2010):

$$\boldsymbol{V_j = 0.5h\ 2\ t_j \frac{b}{s} f_{yi,d} . (\cot\theta + \cot\beta) \sin\beta} \quad \textbf{(5-1)}$$

where:

V_j	The shear strength to be sustained by the steel jacket.
h	The depth of the cross section in the direction of the shear force.
t_j	The thickness of the steel plate.
$f_{yi,d}$	The design yield strength of steel used in the jacket (taken as 270 MPa) divided y partial factor for steel (assumed 1.15)
θ	The strut inclination angle: the assumed inclination of shear crack (safely assumed to be 45^o).

β The angle between the axis of the steel straps and the axis of the member, 90^o in the case of cont nues steel plate.

s The span between each plate, (mm),

b The width of steel plate, (mm), in case of continuous plate : $\frac{b}{s} = 1$,

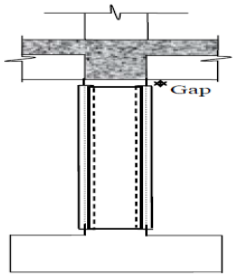

Figure 16: Continuous Steel Jacket of RC Column

In SeismoStruct software (Seismosoft, 2014) the effect of steel jackets are incorporated in the calculation of confinement strength where other automatic calculation of its effect on the lap splices through clamping and shear strength are not currently employed. Some guidelines about the application of steel jacket are suggested such as extending the jacket at least 50% of the lap length (CEN, 2010). Shear strength will be calculated using the above-mentioned formula as per CEN (2010). Since the automatic calculation of shear demands of the original elements are curried out for all inegration sctions[7] at each load increment, the section with minimum capacity (V_{cap}) and maximum demand (V_{dem}) will be selected to calculate the shear provided by the jacket (V_{dem}- V_{cap}). The thickness of the steel plate will be $(t_j = (V_{dem} - V_{cap})/ h\, f_{yi,d})$ where h is the depth of the section parallel to the shear demand for direction of interest as shown in Figure **17**.

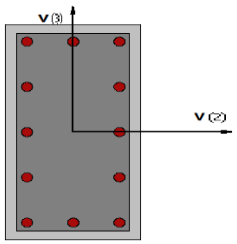

Figure 17: Shear Directions for RC Cross Section (Seismosoft, 2014)

Steel jackets are introduced to enhance the shear capacity of vertical elements for both directions of loading (i.e. pushover analyises directions). Table 13 shows a sample of such calculation where the total capacity for each direction is the shear strength provided by the section itself plus the contribution of the steel jacket as proposed by Equation 5-1.

The steel jackets are not provided to enhance the flexural strength in practice. However, the stiffnesss and strength in the longitudinal direction are instantaneously affected (Fardis, 2009). Buckling of steel plates is expected especially in resisting the cyclic loading even when some moment transferring elements are provided. All of that make such solution not practical - as a lifetime rehabilitation system- espically where many of these retrofitted elements are shear walls loaded in their weak direction in which the local buckling of steel plates is highly expected (Galal and El-Sokkary, 2008).

[7] 5 integration sections are assigned per element.

Table 13: Sample Calculations of Total shear Capacity of steel-jacketed RC Elements along both Shear Axes: Y-Direction model

Element	$V_{dem.}$- V_{cap} *kN*	$h_{(axis),}$ *mm*	$b_{(perp.)}$ *mm*	t_j *mm*	V_j *kN*	V_{tot} *kN*	$V_{cap.}$ *(perp) kN*	$V_{tot.}$ *(perp) kN*
A_a_c	1280.3	1800	300	3	1267.83	1986.50	301.00	512.30
A_b_c	914.69	1800	300	3	1267.83	1987.89	301.00	512.30
A_c_c	996.44	1800	300	3	1267.83	1988.32	301.00	512.30

The use of steel jackets as shown in Figure 18 is mainly for urgent repairing of damaged structures in which immediate reduction of collapse probability is pursued (Fardis, 2009). After building a systematic solution, these elements could be removed or incorporated with other RC repairing as shown by the work of Habahbeh (2015) in which steel corroded plates and I beams were used to build an immediate supporting system for slab after damage by fire. Therefore, it is normally applied to columns where applying steel plates to wall elements needs special care. In case of enhancing the shear strength of beams, other retrofitting technologies could be suggested especially where many of these elements are shallow and hidden. Eurocode 8 (CEN, 2010) emphasizes the use of steel jackets only in columns where no recommendations were made in the case of beams. Many other researchers suggest the use of CFRP materials as an effective alternative of steel as could be seen in the folowing section.

a) Sheet Plate

b) Steel Straps

Figure 18: Steel Jacketing of Columns a) Sheet Plate b) Horizontal Steel Straps

CFRP Sheets/Strips

Unidirectional Carbon fibers are used in which the reinforced fibers are oriented in one direction. The *elastic modulus*, *tensile strength*, manufacturer *layer thickness* and the *ultimate rupture strain* for the selected CFRP from Sika® System Solutions company are 230000 MPa, 3105 MPa, 0.165 mm, and 0.0135 mm/mm, respectively. The design material properties could be calculated by multiplying these values (i.e. ultimate tensile strength and strain) by environmental reduction factor as shown in Table 14 to account for any exposure conditions that FRP materials could sustain. It would be important to limit the number of fiber layers to the minimum because of bonding problems. The maximum number of plies is suggested to be five with any different layer thickness. It was found that the confinement provided by these materials is more sensitive to the tensile strength than the total thickness of CFRP jacket. Three types of FRP materials are shown in the figure, namely: carbon FRP (CFRP), aramid FRP (AFRP) and glass FRP (GFRP).

Wrapping RC elements with CFRP jacket prevents the formulation of plastic hinges and delays bars buckling. In this way, the deformation capacity will be significantly upgraded through confinement. Since CFRP jackets could not continue to the end section (i.e. location of maximum moments), their effect in flexural resistance may be neglected (CEN, 2010). The confinement effect could be automatically calculated by the software. Users are required to assign the properties of FRP materials (CFRP in this study) in the section module of the retrofitted element. For beams, CFRP confinement could not be attained where side bonding schemes are only applicable. This is also the case for lap splice enhancement.

Table 14: Environmental Reduction Factor for Various CFRP Exposure Conditions

Exposure conditions	Environmental reduction factor C_E
Interior exposure	0.95
Exterior exposure	0.85

Unlike providing confinements where full CFRPs jackets are needed, improving the shear capacity of structural member using CFRPs could be effectively attained by different bonding schemes. This is considered a major advantage over strengthening by steel plates where complicated and less effective application methods are needed. Two different bonding schemes will be adopted to enhance the deficiency in shear strength for vertical (i.e. column and shear walls) and horizontal elements (i.e. drop beams). Unidirectional Carbon fibers are used in which the direction of these fibers is oriented in one direction. In the case of beams, these unidirectional fibers are partially applied at the end sections as shown in Figure 19.

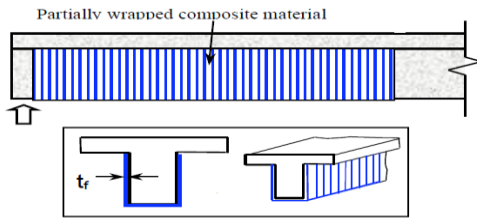

Figure 19: Unidirectional Carbon Fibers Applied at End Sections of Beam (fib, 2006)

The nominal shear strength of a CFRP- strengthened concrete section ($\phi V_n = \phi(V_c + V_s + \psi_f . V_f)$) is evaluated where strength reduction factor (ϕ) is equal 0.75 for shear and torsion (ACI 318, 2014).

The contribution of CFRP reinforcement (V_f) is calculated as the following formula (Equation 5-2) as suggested by ACI 440 (2008) in which the effective stress (f_{fe}) in CFRP could be estimated in much more straightforward procedures than other codes. The contribution of CFRP reinforcement (V_f) is multiplied by the reduction factor (ψ_f) based on different bonding schemes: 0.95 and 0.85 are assumed for fully and three-side wrapping respectively:

$$\boldsymbol{V_f = A_{fv}.f_{fe}.(\sin\alpha + \cos\alpha).\frac{d_{fv}}{s_f}} \quad \textbf{(5-2)}$$

where:

- V_c Nominal shear strength provided by concrete with steel flexural rein orcement, (N),
- V_s Nominal shear strength provided by steel stirrups, (N),
- V_f Nominal shear strength provided by CFRP stirrups, (N),
- A_{fv} The area of CFRP shear reinforcement with spacing S_f, (mm^2), $A_{fv} = 2nt_f w_f$,
- n Number of CFRP p ies,
- t_f The thickness of the CFRP sheet, (mm),
- S_f The span between each sheet, (mm),
- w_f The width of FRP reinforcing plies, (mm), for CFRP sheets: $\frac{w_f}{s_f} = 1$,
- d_{fv} Effective depth of FRP shear reinforcement, (mm),
- α The angle between the fiber direction in the CFRP strip and the axis of the member,
- b_w Web width of the section, (mm),
- d The distance from extreme compression fiber to centroid of tension reinforcement, (mm),
- h Overall thickness or height of a member, (mm), $h, d, \alpha, w_f, d_{fv}, b_w and\ s_f$ (mm) are shown in Figure 20,
- f_{fe} Effective stress in the FRP; stress level attained at section failure, (MPa), $f_{fe} = \varepsilon_{fe}.E_f$,
- E_f tensile modulus of elasticity of FRP, (MPa),
- ε_{fe} The effective strain in CFRP laminates, $\varepsilon_{fe} = 0.004 \leq 0.75\varepsilon_{fu}$ for fully wrapping and $\leq \kappa_v.\varepsilon_{fu}$ for U − jacket,
- κ_v Bond-dependent coefficient for shear, $\kappa_v = \frac{k_1 k_2 L_e}{11{,}900\ .\varepsilon_{fu}}$,
- L_e Active bond length of FRP laminate, (mm), $L_e = \frac{23{,}300}{(n.t_f.E_f)^{0.58}}$,
- k_1 Modification factor applied to κ_v to account for concrete strength, $k_1 = \left(\frac{f_c}{27}\right)^{2/3}$
- k_2 Modification factor applied to κ_v to account for wrapping scheme, $k_2 \text{for U} - \text{wraps} = \frac{d_{fv} - Le}{d_{fv}}$,
- ε_{fu} Design rupture strain of FRP reinforcement, (mm/mm), $\varepsilon_{fu} = \varepsilon^*_{fu} \times C_E$, and
- ε^*_{fu} Ultimate rupture strain of FRP reinforcement, (mm/mm).

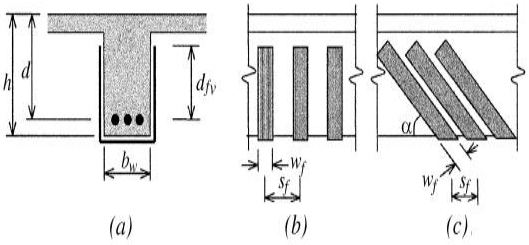

Figure 20: Variables used in Shear Strength Calculation of CFRP- Strengthened RC Elements (ACI 440, 2008)

The increase in strength needed (ΔV_u) is the difference between the demand and capacity of the original cross section that could be directly calculated by the software.

These elements are shear walls as could be seen in the same table. It should be clear that the nonlinear interaction of flexural and shear are not incorporated in our model, hence, the flexural response of CFRP retrofitted structure will not be changed except if such retrofitting comes to enhance the deformation capacity (i.e. the ductility) by confinement as discussed in the following paragraphs.

Table 15: Shear Strength Calculation: Number of CFRP Plies for Column Jacket

Elements-Shear Axis	ΔV_u, kN	d_{fv}, mm	n	t_{total},mm
A_a_c-axis(3)	1280	1800	4	0.66
A_b_c-axis(3)	914.67	1800	3	0.495
A_c_c-axis(3)	996.44	1800	3	0.495
A_d_c-axis(3)	634.48	1800	2	0.33

For external drop beams with CFRP U-jacket, the number of plies ($\boldsymbol{n}$) is calculated by evaluating the required shear contribution $\left(\boldsymbol{V_{f,req}} = \frac{\Delta \boldsymbol{V_u}}{\phi \boldsymbol{\psi_f}} = \boldsymbol{113 \,.\, \varepsilon_{fe} . n \,.\, d_{fv}}\right) (\boldsymbol{N, mm})$ as shown in Table 5-5.

It would be important to emphasize that the enhancement of ductility (i.e. deformation capacity) through confinement is only generated when CFRPs are fully wrapping the RC cross-section by orienting the fibers perpendicular to the longitudinal axis. Hence, the confinement strength calculated by the software will be considered for columns and shear walls where it is possible to introduce jackets. As a result, the fracture strain of concrete core remains as before retrofitting for horizontal elements. One could see the effect of confinement provided by CFRP jackets in Figure 21. The major advantage of such issue is that the strong column- weak beam approach is surely attained[8]. On the other hand, excessive fracture of these elements could not be resolved with this retrofitting strategy. It could be more critical if the local collapse due to fracture of many elements is possible. Since the advantage of introducing CFRP jackets is to delay the formulation of concrete core fracture, it would be important to evaluate the confined concrete compressive strength (f'_{cc}) and the fracture strain (ε_{ccu}) for jacketed members as shown in Figure 21. The definition of fracture strain (ε_{ccu}) at ($0.85f'_{cc}$) will be implemented as developed in ACI 440 (2008).

Table 16: Shear Strength Calculation: Number of CFRP Plies for Beam U- Jacket

Elements	ΔV_u (kN)	d_{fv} (mm)	k_2	k_1	n_i	L_e (mm)	κ_v	ε_{fe}	n
B1	97.09	260	0.88	0.95	2.38	31.12	0.15	2.19E-03	2
B2	145.26	260	0.92	0.95	5.3	19.56	0.10	1.44E-03	5

[8] By confining the vertical elements only.

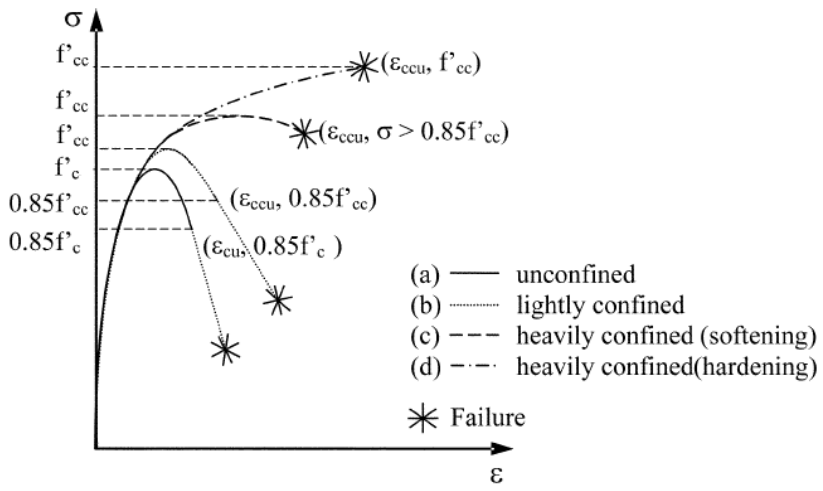

Figure 21: Stress- Strain Behavior of Confined and Unconfined RC Elements (ACI 440, 2008)

As discussed in the introductory section of this chapter, the assumption of fracture strain of concrete core was little above the usable strain for unconfined RC section under combined loading. The validity of such assumption comes from the fact that the confinement factors for almost all sections are identical and almost equal one. ACI 440 (2008) recommends that the effect of CFRP confinement should be ignored for rectangular sections with aspect ratios (*h/b*) exceeding two. In this case study, the majority of columns and shear walls have aspect ratios equal or greater than two. On the other hand, no special recommendations for such issue are seen in Eurocode 8 Part 3 (CEN, 2010). In fact, it is obvious that the confinment factors calculated for these elements are relativily small and do not change significantly with changing the confinment thickness as shown in Table 17 in which the effect of two layers of CFRP jacket are invistigated for different shapes of column cross sections. The model of Mander et al. (1989) is adopted for calculating the confinemt factors.

Table 17: Confinement Factors for Different Shapes of Column Elements with and without CFRP

Element Shape	Cross Section (mm)	Confinement factor		
		Original Section	CFRP Jacket	% Increase
Circular	750	1.115[9]	1.53	37%
Square	750	1.02	1.12	9.8%
Rectangular[10]	600 × 300	1.01	1.07	6%

[9] Circular hoops
[10] With aspect ratio equal 2.

Consequently, designing a CFRP strengthening scheme to provide confinement around rectangular shaped columns (with aspect ratio greater than 2) could not be an efficient alternative. The effect of CFRP layers on the deformation capacity and ductility could be seen by evaluating the section's confinement factor for vertical elements before and after introducing two layers of CFRP jacket. It was clear that the contributions of such jackets are very small and negligible.

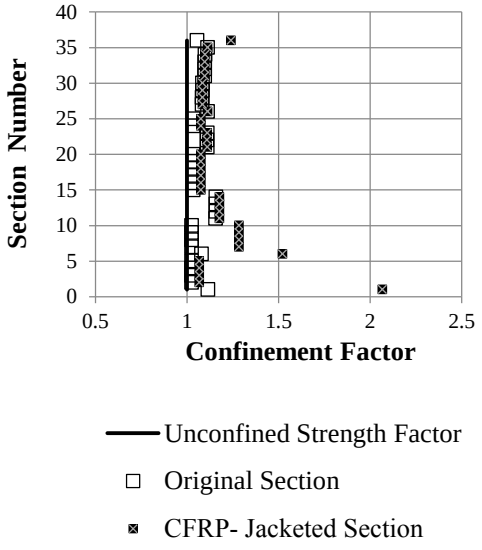

Constructing New Shear Walls

The structural system is asymmetric in stiffness and mass along both directions. So, as we trying to lessen the irregularity in stiffness (since altering the mass distribution is not possible), a new distribution of stiffness could be achieved by reducing the difference between the displacement of the opposite corners as shown in Figure 22 (i.e. δ_1 and δ_2). Stiffening the flexible side is another meaning of such equilibrium of stiffness distribution. This balance could be easier to achieve in regular shaped buildings (i.e. rectangular or square). In other words, altering the stiffness for these buildings is more achievable since the mass is symmetric about the principal axes.

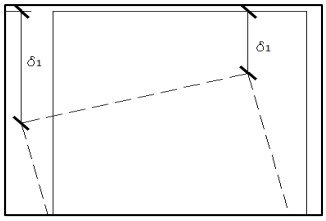

Figure 22: Torsional Response Concept

In our case, the procedure is more difficult and more time consuming especially if one would run the Eigenvalue analysis for each single trial to check the mass participation along both directions. Translational response resulting from static procedures is less divergent from what is expected under actual earthquakes. These procedures are not able to capture the torsional behavior. Based on that and by building some rational interpretation from the original eigenvalue analysis results, trial and error procedures were performed to choose the proper location of these new shear walls trying to (1) adopt the preferable schemes and to (2) get the desired translational response along both directions.

Some preferable schemes of shear wall distributions are shown in Figure 23a and b, where constructing shear walls within the perimeters (far away from the corners) would be more practical. One of the possibilities is generated in Figure 24 and 25. The size of these walls is different as shown in the same figure where the thickness is 300 mm. The transverse, ρ_l and longitudinal reinforcement[11], ρ_t are equal (0.004) (Φ12/ 150 *mm*). Normal strength concrete is chosen for the new elements where other properties of workability should be carefully calibrated. The compressive strength of reinforced concrete is taken as 35 MPa where the tensile strength of reinforcing bars is 420 MPa.

[11] Shall not be less than 0.0025 (ACI 318, 2014).

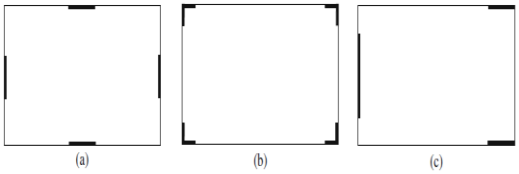

Figure 23: Some Arrangements of Shear Walls (Fardis And Springer Link Online Service, 2009)

It is worth to mention that Part A and B of the structural plan in Figure 25 are not continuing to the roof floor as shown in Figure 24a, and b. These two parts of the structure have less contribution to the lateral resistance of the structure. Some elements in Part B are not connected with slab as shown in Figure 24b. It would be the reason behind the need for like 10 mode shapes to capture a 90% of the mass. Columns have small cross sectional dimensions compared with shear walls as shown in Figure 25.

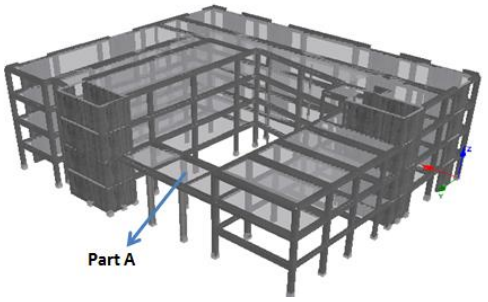

a)

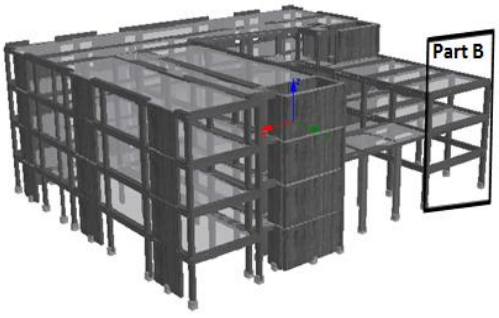

b)

Figure 24: Shear Wall Retrofitted Model a) Part A and b) Part B

Eigenvalue analysis results are shown in Table 18. The fundamental periods are substantially reduced for both principal directions. More mass participation percentages are generated along X direction. Comparing these values with the original eigenvalue analysis results for rigid diaphragm model as shown in Table Error! No text of specified style in document.**4**, the torsional mode of vibration along X direction is almost vanished with 67% of translational mass compared with 29% for the original one. Mode shapes and associated periods of vibration for both directions are listed in Table 19.

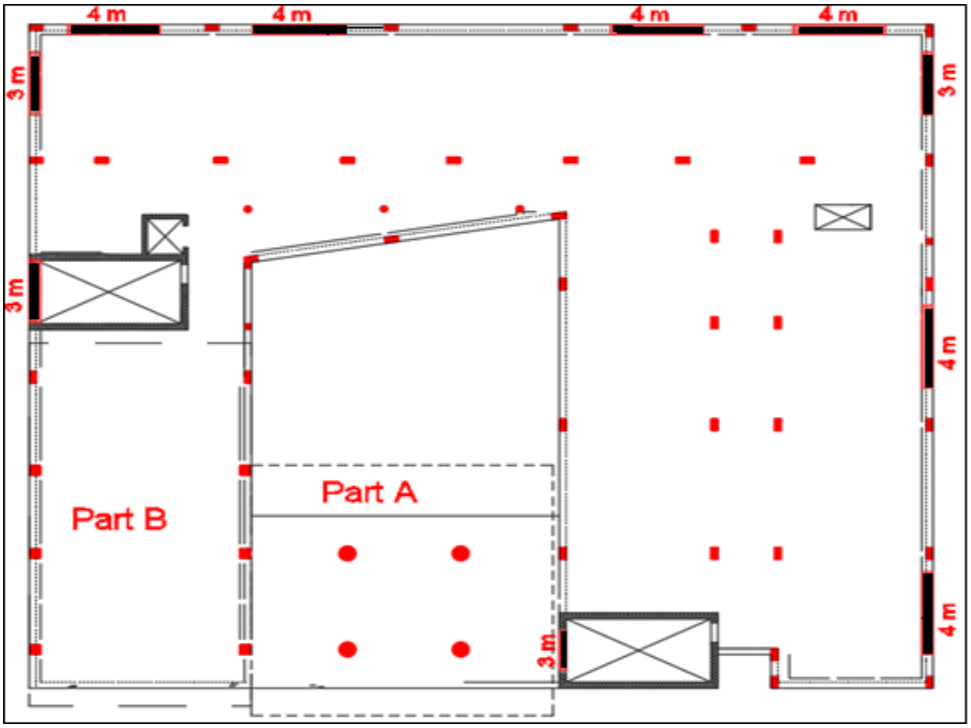

Figure 25: Selected Shear Wall Retrofitted Structure

Table 18: Results of Eigenvalue Analysis of Shear Walls-Retrofitted Structure

Mode	Period (sec.)	Mass participation %		
		X	Y	Z
1	0.24	0.32%	**73.99 %**	1.63 %
2	0.17	**67.25%**	1.04 %	6.49 %
3	0.14	5.97%	1.81 %	68.13 %
4	0.10	0.34%	0.00 %	0.24 %

Table 19: Mode Shapes and Associated Periods of retroffited structure

Mode Number	Direction	Cumulative Mass Percentages	Period of Vibration (sec.)
1	Y	73.99%	0.24
2	X	67.25%	0.17

The suggested shear wall distribution is further examined using ETABS® 2015 software in which the centers of mass and resistance are evaluated. The model is shown in Figure 26. The results show very small values of eccentricities along both directions for all floors as shown in Table 20. As a result, the main objective of lessening the existing irregularities by the global intervention is remarkably met.

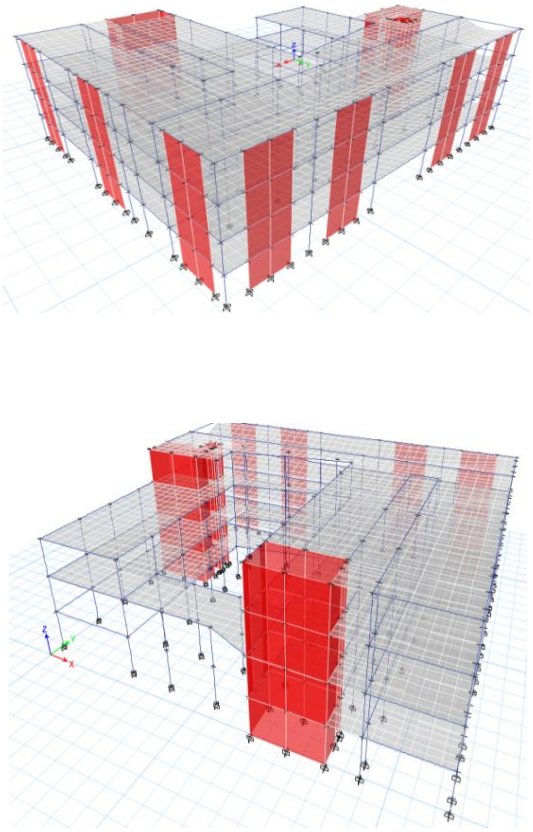

Figure 26: Shear Wall- Retroffeted Model Using ETABS® 2015

Table 20: Centers of Mass and Resistance of Shear Wall-Retrofitted Model using ETABS® 2015

	Static eccentricity	
Story Diaphragm	e_x	e_y
	m	m
Story4	1.98	1.68
Story3	0.23	1.18
Story2	1.29	0.90
Story1	2.36	0.69

e_x Static eccentricity in X –direction.
e_y Static eccentricity in Y –direction.

Following the procedure of evaluating the performance points, the structural performance measures in terms of material strains and chord rotations for both the original and retrofitted structure along X and Y directions are shown in Figure 27 and Figure 29, respectively. It is obvious that the effect of such global interventions on the flexural demands (i.e. steel yielding and concrete fracture) is highly recognized. It seems that the structure remains elastic for almost the entire seismic demand (i.e. until the performance point). However, Columns are absorbing more demands to let them start yielding before beams but their strength is maintained during the analysis and even after crushing of many beams. Roof displacements and interstory drift ratios are compared with corresponding values of the original structure in Figure 28 and Figure 30 for X and Y directions, respectively. The figure proves the efficiency of shear walls in limiting these values to very acceptable limits.

These new shear walls not only enhance the global structural response, but they also reduce the seismic demands on local elements. Shear demands imposed by gravity loads are also reduced for some elements by shortening the span length as could be seen in Figure **25**. In additions, existing elements could now be treated as secondary elements in which less demanding shear and chord rotation capacity acceptance criteria are implemented (Fardis, 2009).

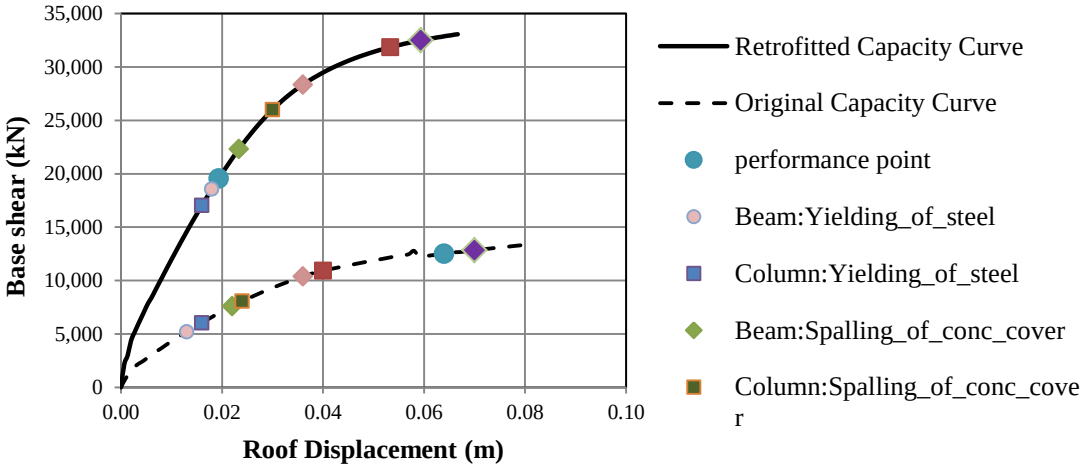

Figure 27: Structural Performance for the Original and Shear Wall-Retrofitted Model: X-direction

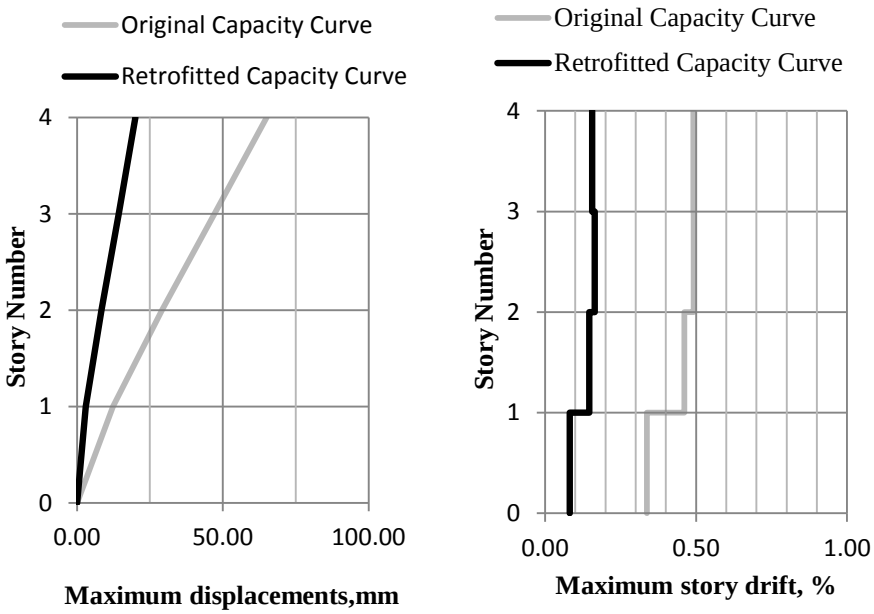

Figure 28: The Maximum Global Displacements and Interstory Drifts at the Performance Point for the Original and Shear Wall-Retrofitted Model: X-Direction

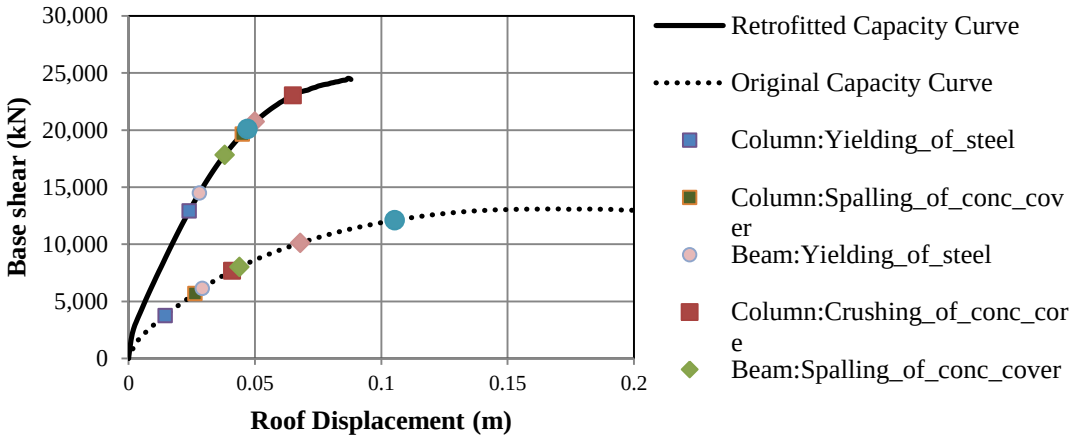

Figure 29: Structural Performance for the Original and Shear Wall-Retrofitted Model: Y-direction

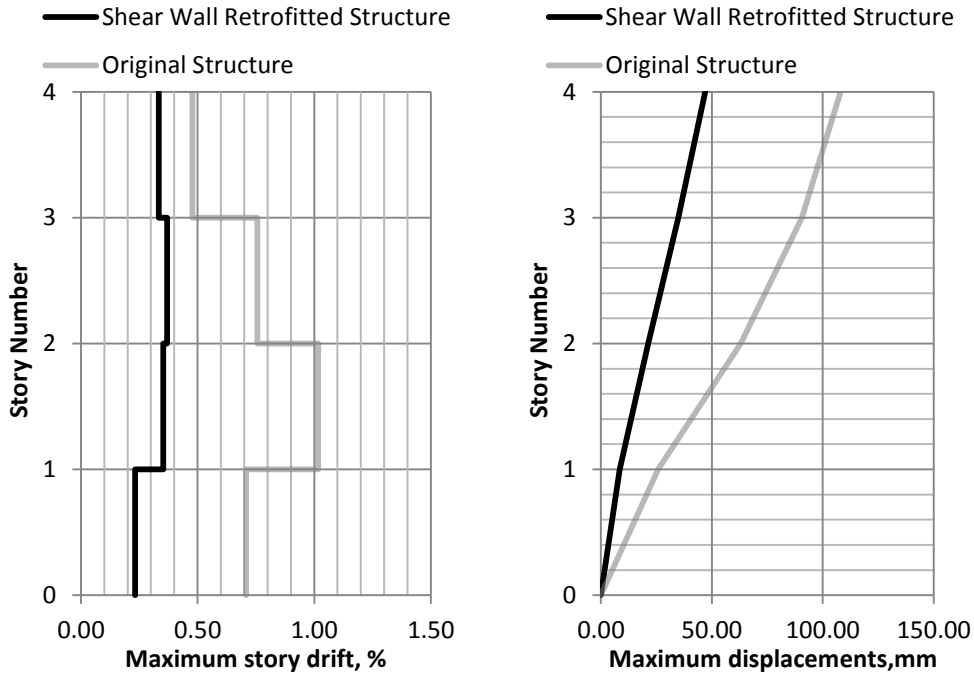

Figure 30: The Maximum Global Displacements and Interstory Drifts at the Performance Point for the Original and Shear Wall-Retrofitted Model: Y-Direction

Results and Conclusions

This study shows the effectiveness of the global retrofitting methodologies in upgrading the entire seismic performance of the school building. Constructing new shear walls limits the interstory drifts and reduces the seismic demands on local elements. It also shows the effectiveness of CFRP jackets in enhancing the shear capacity as a main function of these materials for vertical elements. The contribution of CFRP jackets is almost negligible in providing confinement around rectangular shaped cross sections with aspect ratio greater than two. CFRP jackets are also used at end sections of drop beams to strengthen their resistance to shear. However, for such uses described previously, carbon FRP jackets are much lighter, easier to install and more effective than steel-strengthening methods. The latter is also not practical as a jacket around rectangular sections and their bonding to existing substrata are questionable. Considering the suggested local intervention methods, comparison between materials cost of steel and carbon FRP jackets is presented in Table 21 for column element (i.e. A_A_C_58). The higher cost of FRP materials is offset by reduced labor costs and installing equipment. It also minimizes the downtime during the installation process, making them a more cost-effective retrofitting technology than traditional strengthening of steel jacketing. However, the study shows that these methods fail to achieve the performance level in which stiffness strengthening is needed.

Table 21: Cost Comparison between CFRP and Steel Plates for Column Element: A_A_C_58

	CFRP	Steel Plates
t_{total}, mm	0.66	3
Volume , m^3	0.0097	0.0459
Specific Weight, kN/m^3	20	78
Cost per kg	30	1
Total Weight, Kg	19	358.7
Cost $	582	358

It would be important to evaluate the shear capacity in a brief discussion. As could be seen in a, selected area (Area A) from the slab diaphragm is considered. Since the behavior of one way slab systems is to distribute the dead (D) and live (L) load on two supporting perpendicular beams, the gravity load combination (*1.2D +1.6L =15 kN/m²*) is evaluated for beam with section (A-A). The shear strengths[12] provided by concrete (V_c) and transverse reinforcement (V_s) are ($0.167\sqrt{f'_c}\, b_w\, d = 135\ kN$) and ($A_V . f_{vy} . \frac{d}{s} = 152\ kN$), respectively. The transverse shear strength is taking into account the shear reinforcement[13] provided for the entire height of the section (i.e. by taken A_v equals 2 A_{vb} not 4 A_{vb}). This simple calculation shows that the demand shear (V_u/ϕ= *307 kN*) is more than the strength provided by both concrete and transverse reinforcement ($V_c + V_s$ *=287 kN)* where:

[12] Assuming pure shear action, axial and flexure actions would be incorporated in other formulas of ACI 318 (2014).
[13] The area of one leg.

D	Dead load value (kN/m^2),
L	Live load value (kN/m^2),
f'_c	The compre sive strength of concrete (MPa),
b_w	Web width, or diameter of circular section (mm),
d	Distance from extreme compression fiber to centroid of tension reinforcement (mm),
A_V	Area of shear reinforcement spacing s (mm^2),
f_{vy}	Specified yi ld strength of transverse reinforcement (MPa),
s	Center-to-center spacing of transverse reinforcement (mm),
A_{vb}	Area of single bar of reinforcement (mm^2),
V_u	Factored shear force at section (kN)
ϕ	Strength reduction factor for shear.

Despite such conservative computation, this could be more critical with the demanding provisions in recent seismic evaluation codes of existing buildings. This problem is resolved in beams with section B-B as shown in b (i.e. Area B). Such beams with good depth to width ratio maintained shear capacity during the analysis. It is worth mentioned that these two section are sustaining the same value of ultimate load per unit length with slight increase for section A-A (i.e. the shear deficient section) but the length of beams with section B-B is 500 mm longer than that for section A-A.

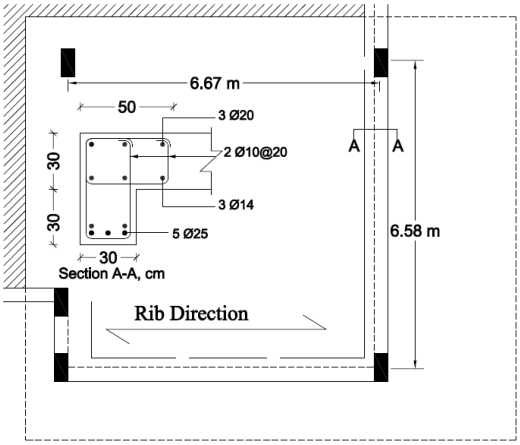

a) Area A

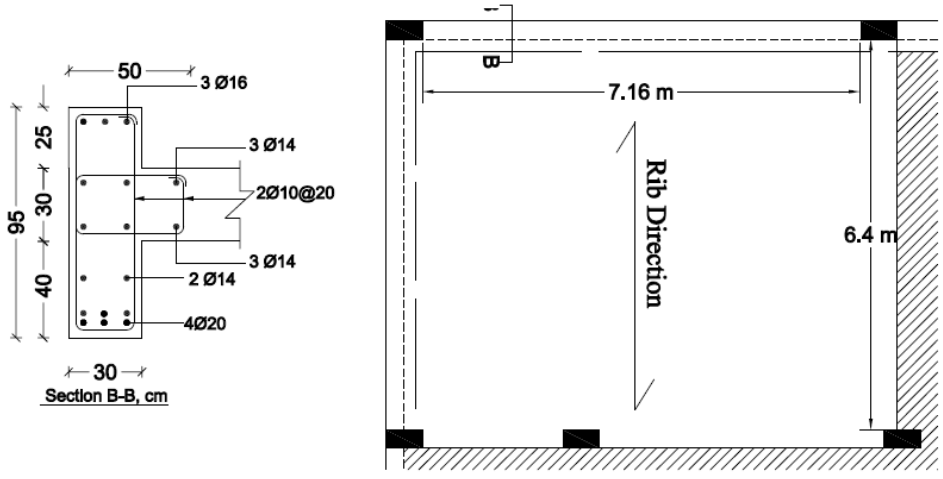

b) Area B

Figure 31: Selected Areas in Slab Diaphragm

Further work

Rehabilitation and retrofitting for upgrading the seismic behavior of existing buildings should be carried out after determining the deficiencies with care. Seismic assessment of existing buildings is a divergent subject since it incorporates the theory-based approaches in modeling and analyzing actual structures. International programs should be established to ensure that these modeling assumptions could fit the theory in a compromising accuracy. Further works and intensive studies for the following topics are highly suggested:

1. The validity of rigid diaphragm assumptions in modeling one-way slab structure could be an important issue to address. The torsional behavior of the school is remarkably seen in such modeling approach leads to, as not expected, much lesser capacity when compared with equivalent truss model. Modeling the slab as a rigid diaphragm in irregular shaped structure unrealistically reduces the structural response in terms of torsional stiffness, causing large torsional deformations (Computers and Structures Inc. , 2000).
2. SeismoStruct (Seismosoft, 2014) software is taking into account the reinforcement steel fibers in constructing the structural capacity and local elements actions. Such effect could be explored using other commercial software in which the conventional plastic hinge analysis is still adopted.
3. Since the study employed the nonlinear static analysis, the global ductility capacities (μ) are directly extracted from the displacement-force capacity curve without introducing any overstrength factors (*R*) specified in design codes. It would be important to examine the suggested values of these factors and compare it with the actual ductility capacity resulting from nonlinear analysis procedures. The suggested overstrength reduction factor is 3.5 for ordinary moment-resisting frames. The corresponding ductility could be evaluated by different formulas available in literature, since the direct relationship between these factors ($R = f_n(\mathrm{T}, \mu)$) holds.
4. Evaluating the current conditions of the school building is a highly important subject to be addressed. The study discusses seismic upgrading methods of sound structures where repairing to gain the resistance under gravity loads is not covered. Any failure of structural elements should be repaired and strengthened by proper methods such as RC jacketing.
5. Incorporation of the following aspects in the study could be further investigated:
   a. Modeling of ramped slabs.
   b. Considering different levels of confidence factors since the study implement a confidence factor of one (CEN, 2010).
   c. The failure mechanism of member or structure by observing the location of hinges formulated along the member.
   d. The connection of new shear walls to existing structural elements. The study assumes rigid links to the surrounding diaphragm where other assumptions could be investigated.
6. The assessment of the school building is carried out using the conventional nonlinear static analysis where the horizontal load pattern is constant and based on the considered fundamental mode. The recent adaptive pushover

analysis could be explored to draw a comparison. In the latter, the load pattern is updated taking into account the change in stiffness at each load increment.

7. Introducing the performance engineering methodology in our design practice. It would be important to verify the design of new buildings using the performance design engineering concepts.

REFERENCES

Abdel-Jaber, M. S., Shatanawi, A. S., and Abdel-Jaber, M. S. (2007). Guidelines for Shear Strengthening of Beams Using Carbon Fibre-Reinforced Polymer (FRP) Plates. **Jordan Journal of Civil Engineering**. 1(4), 327-335.

ACI 318. (2014). Building Code Requirements for Structural Concrete and Commentary. **American Concrete Institute**. Farmington Hills.

ACI 440. (2008). Guide for the Design and Construction of Externally Bonded FRP Systems for Strengthening Concrete Structures (ACI 440.2R-02). **American Concrete Institute**. Farmington Hills, Michigan.

Al-Dwaik, M. M., and Armouti, N. S. (2013). Analytical Case Study of Seismic Performance of Retrofit Strategies for Reinforced Concrete Frames: Steel Bracing with Shear Links versus Column Jacketing. **Jordan Journal of Civil Engineering**. 7(1), 26-43.

Armouti, N. S. (2003). Response of Structures to Synthetic Earthquakes. **The 9th Arab Structural Engineering Conference**. Abu Dhabi, UAE, (pp. 331-339).

American Society of Civil Engineers (ASCE), (2005). ASCE/SEI Standard 7-05, Minimum Design Loads for Buildings and Other Structures (10 ed.). **American Society of Civil Engineers**. Reston, VA.

American Society of Civil Engineers (ASCE), (2003). **Seismic Evaluation of Existing Buildings** (ASCE/SEI 31-03). Reston, Virginia.

ATC, (1996). Seismic Evaluation and Retrofit of Concrete Buildings. **ATC 40, Applied Technology Council**. Redwood City, CA.

Basu, D., and Jain, S. K. (2004). Seismic Analysis of Asymmetric Buildings with Flexible Floor Diaphragms. **American Society of Civil Engineers**. 130(8), 1365-1389.

Beyer, K., Dazio, A., and Priestley, M. N. (2008). Elastic and Inelastic Wide-Column Models for RC Non-Rectangular Walls. **The 14th World Conference on Earthquake Engineering WCEE.** Beijing, China.

Casarotti, C., and Pinho, R. (2006). Seismic Response of Continuous Span Bridges through Fibre-Based Finite Element **Analysis. Journal of Earthquake Engineering and Engineering Vibration**. 5(1), 119-131.

CEN. (2003). European Standard EN 1998-1 Eurocode 8: Design of Structures for Earthquake, Part 1: General Rules, Seismic Actions and Rules for Buildings. **Comite Europeen de Normalisation**. Brusells.

CEN. (2010). European Standard EN 1998-3 Eurocode 8: Design of Structures for Earthquake Resistance Part 3: Assessment and Retrofitting of Buildings. **Comite Europeen de Normalisation**. Brussels.

Computers and Structures Inc., **SAP 2000 Standard User's Manual**, Version 17.1, 2013.

Correia, A. A., and Virtuoso, F. E. (2006). Nonlinear Analysis of Space Frames. In C.A. Mota Soares et.al. (Ed.). **The 3rd European Conference on Computational Mechanics Solids, Structures and Coupled Problems in Engineering**. Lisbon, Portugal. (pp. 5–8).

Deierlein, G. G., Reinhorn, A. M., and Willford, M. R. (2010). Nonlinear Structural Analysis For Seismic Design NEHRP, Seismic Design Technical Brief No. 4;. Produced by the NEHRP Consultants Joint Venture, a Partnership of the Applied Technology Council and the Consortium of Universities for Research in Earthquake Engineering. Gaithersburg: **the National Institute of Standards and Technology**, MD, NIST GCR 10-917-5.

Deierlein, G. G., and Kaul, R. (2001). Methodology and Simulation Models For Performance Based Earthquake Engineering. Seattle, Washington: **The 3rd U.S.-Japan Workshop on Performance-Based Earthquake Engineering Methodology for Reinforced Concrete Building Structures**. Seattle, Washington.

Elnashai, A. S., and Izzuddin, B. A. (1993). Modelling of Material Non-Linearities in Steel Structures Subjected to Transient Dynamic Loading. **Earthquake Engineering and Structural Dynamics**. 22(6), 509-532.

Erberik, M. A., and Kurtman, B. (2010). A Detailed Evaluation on Degrading Behavior of Structural Systems. **Proceedings of the 9th U.S. National and 10th Canadian Conference on Earthquake Engineering**, Toronto, Ontario, Canada. (p. Paper No 369).

Fardis, M. N., and Springer Link Online Service. (2009). **Seismic design, assessment and retrofitting of concrete buildings: Based on EN-eurocode 8**. Dordrecht: Springer Netherlands.

FEMA 154. (2002). Rapid Visual Screening of Buildings for Potential Seismic Hazards. **Federal Emergency Management Agency**. Redwood City, California.

FEMA 356. (2000). Prestandard and Commentary for Seismic Rehabilitation of Buildings. **Federal Emergency Management Agency**. Reston, Virginia.

FEMA 440. (2005). Improvement of Nonlinear Static Seismic Analysis Procedures, FEMA Report 440. **Federal Emergency Management Agency**. Washington.

FEMA P-58. (2012). Seismic Performance Assessment of Buildings. **Federal Emergency Management Agency.** Washington, D.C.

Ferracuti , B., and Savoia, M. (2005). Cyclic Behavior of FRP-Wrapped Columns under Axial and Flexural Loadings. **Proceedings of the International Conference on Fracture**. Turin, Italy.

Ferracuti, B., Savoia, M., Francia, R., Francia, R., Pinho, R., and Antoniou, S. (2007). Push-Over Analysis of FRP-Retrofitted Existing RC Frame Structures. Greece: **University of Patras**.

fib. (2006). Retrofitting of concrete structures through externally bonded FRPs, with emphasis on seismic applications. fib Bulletin 35, **Federation Internationale du Beton**. Istanbul and Ankara.

Folić, R. (2015). Performance Based Seismic Design of Concrete Buildings Structures – Bases. **The 41th Anniversary Faculty of Civil Engineering Subotica**. Contemporary Achievements in Civil Engineering. Subotica, Serbia.

Fragiadakis, M., and Papadrakakis, M. (2008). Modeling, analysis and reliability of seismically excited structures: Computational issues. **International Journal of Computational Methods.** 5(5), 1-30.

Fragiadakis, M., Pinho, R., and Antoniou, S. (2008). Modeling inelastic buckling of reinforcing bars under earthquake loading. In M. Papadrakakis, D. C. Charmpis, and N. D. Lagaros (Ed.), **in Progress in Computational Dynamics and Earthquake Engineering. Netherlands: Taylor and Francis**.

Galal, K., and El-Sokkary, H. (2008). Recent Advancements in Retrofit of RC Shear Walls. **The 14th World Conference on Earthquake Engineering**. Beijing, China.

Ghobarah, Ahmed and Youssef, Maged (2000). Rehabilitation of RC Buildings Using Structural Walls. **The 12th World Conference on Earthquake Engineering**. Newzeland.

Govalkar, V., Salunke, P. J., and Gore, N. G. (2014). Analysis of Bare Frame and Infilled Frame with Different Position of Shear Wall. **International Journal of Recent Technology and Engineering (IJRTE)**. 3(3), 67-72.

Habahbeh, S. (2015). AL-Bukharia Fire: Urgent Rehabilitation Works. **The Sixth Jordanian International Civil Engineering Conference (JICEC06)**. Jordan Engineers Association (JEA). Amman.

IBC. (2009). International Building Code. **International Code Council**, INC. U.S.A.

JNBC. (2006). Jordanian Code for Loads and Forces. **The Jordan National Building Council**. Amman.

Jun, Dae-Han (2014). Nonlinear Analysis of Reinforced Concrete Shear Wall Using Fiber Elements. **Proceedings of the 9th International Conference on Structural Dynamics**. Porto, Portugal.

Khalifa, A., Gold, W. J., Nanni, A., and M.I., A. (1998). Contribution of Externally Bonded FRP to Shear Capacity of Flexural Members. **ASCE-Journal of Composites for Construction**, 2(4), 195-203.

Maity, S., Singha, K., and Singha, M. (2012). Textiles in Earth-Quake Resistant Constructions. **Journal of Safety Engineering**, 1(2), 17-25.

Mpampatsikos, V., Nascimbene , R., and Petrini, L. (2014). A Critical Review of the R.C. Frame Existing Building Assessment Procedure According to Eurocode 8 and Italian Seismic Code. **Journal of Earthquake Engineering**, 12(S1), 52–82.

Mander, J. B., Priestley, J. N., and Park, R. (1989). Theoretical Stress-Strain Model for Confined Concrete. **The ASCE Journal of Structural Engineering**. 114(8), 1804-1826.

Martinez-Rueda, J. E., and Elnashai, A. S. (1997). Confined concrete model under cyclic load. **Materials and Structures**. 30(197), 139-147.

Mpampatsikos, V. (2008). A Critical Review of the R.C. Frame Existing Building Assessment Procedure According to Eurocode 8 and Italian Seismic Code, **MSc Dissertation.** European School for Advanced Studies in Reduction of Seismic Risk.

Nabil F. Grace and S. B. Singh (2005). Durability Evaluation of Carbon Fiber-Reinforced Polymer Strengthened Concrete Beams: Experimental Study and Design. **ACI Structural Journal.** 102(1), 40-53.

Naito, C. J., Moehle, J. P., and Mosalam, K. M. (2001). Experimental and Computational Evaluation of Reinforced Concrete Bridge Beam-Column Connections for Seismic Performance. **Pacific Earthquake Engineering Research Center (PEER).** California, Berkeley.

Nicknam, A., Ahmadi, H. R., and Mah, N. (2008). A comparative study of the traditional performance and The Incremental Dynamic Analysis approaches (IDA). **The 14th World Conference on Earthquake Engineering**. Beijing, China.

Pinho, R. (2000). Selective retrofitting of RC structures in seismic areas, **PhD Thesis**. London, UK: Imperial College.

Priestley , M. N., and Grant, D. N. (2005). Viscous Damping in Seismic Design and Analysis. **Journal of Earthquake Engineering**, 9(2), 229–255.

Seo, J., Hu , J. W., and Davaajamts, B. (2015). Seismic Performance Evaluation of Multistory Reinforced Concrete Moment Resisting Frame Structure with Shear Walls. **Sustainability**, 7(1), 14287-14308.

Sakino, K., and Sun, Y. (2000). Steel Jacketing for Improvement of Column Strength and Ductility. **The 12th World Conference on Earthquake Engineering**. Newzeland.

Seismosoft. (2014). SeismoStruct v7.0 – A computer program for static and dynamic nonlinear analysis of framed structures. available from **http://www.seismosoft.com**.

Seismosoft. (2016). "SeismoMatch 2016 – A computer program for spectrum matching of earthquake records," available from **http://www.seismosoft.com**.

Seo, J., Hu, J. W., and Davaajamts, B. (2015). Seismic Performance Evaluation of Multistory Reinforced Concrete Moment Resisting Frame Structure with Shear Walls. **Sustainability**. 7, 14287-14308

Sousa R., Bianchi F., Pinho R., Nascimbene R. (2011). Modelling issues on seismic assessment of irregular RC structures. **Proceedings of the 3rd International Conference on Computational Methods in Structural Dynamics and Earthquake Engineering (COMPDYN 2011)**, Corfu, Greece. 25–28.

Sousa R., Kazantzidou-Firtinidou D., Sousa L., Kohrangi M., Eroglu T., Pinho R., Nascimbene R. (2012). Effect of Different Modeling Assumptions on the Seismic Response of RC Structures. **15th World Conference on Earthquake Engineering, WCEE 2012**. Lisbon, Portugal, 24-28.

Spoelstra, M. R., and Monti, G. (1999). FRP-Confined Concrete Model. **Journal of Composites for Construction.** 3(3), 143-150.

Teng, J., Lam, L., and Chen, J.-F. (2004). Shear Strengthening of RC beams with FRP Composites. **Progress in Structural Engineering and Materials**. 6(3), 173–184.

Thermou, G., and Elnashai, A. (2008). Seismic retrofit schemes for RC structures and local–global consequences. **Journal of Earthquake Engineering**. 8(1), 1–15.

UBC. (1997). Uniform Building Code. **International Council of Building Officials**. Whittier, California

UNDP Jordan. (2009). Disaster Risk Management Profile (Amman- Jordan). **Support to Building National Capacities for Earthquake Risk**. Amman.

Varum, H. (2003). Seismic Assessment, Strengthening and Repair of Existing Buildings. **PhD Thesis**, University of Aveiro, Portugal.

Wilson, E. L. (2004). Static and Dynamic Analysis of Structures. **Computers and Structures**, Inc. Berkeley, CA.

Yeh, F.-Y., and Chang, K.-C. (2004). Size and Shape Effect on FRP Confinements for Rectangular Concrete Columns. **The 13th World Conference on Earthquake Engineering**. Vancouver, B.C., Canada.

Yılmaza, N., and Yücemenb, S. M. (2015). Sensitivity of Seismic Hazard Results to Alternative Seismic Source and Magnitude-Recurrence Models: a Case Study for Jordan. **Geodinamica Acta**, 27(2-3), 188–201.

Yu, W. (2006). Inelastic Modeling of Reinforcing Bars and Blind Analysis of the Benchmark Tests on Beam-Column Joints under Cyclic Loading. **MSc Dissertation**, ROSE School. Pavia, Italy.